Post-Monsoon Pollution Events in the Indo-Gangetic Plain Using 18 Years [2007–2024] of IASI Carbon Monoxide Satellite Measurements

Selviga Sinnathamby, Sarah Safieddine, Marie Doutriaux-boucher, Pierre Coheur, Cathy Clerbaux

▶ **To cite this version:**

Selviga Sinnathamby, Sarah Safieddine, Marie Doutriaux-boucher, Pierre Coheur, Cathy Clerbaux. Post-Monsoon Pollution Events in the Indo-Gangetic Plain Using 18 Years [2007–2024] of IASI Carbon Monoxide Satellite Measurements. Journal of Geophysical Research: Atmospheres, 2026, 131 (4), pp.e2025JD044219. ⟨10.1029/2025jd044219⟩. ⟨hal-05519340⟩

HAL Id: hal-05519340

https://hal.science/hal-05519340v1

Submitted on 19 Feb 2026

HAL is a multi-disciplinary open access archive for the deposit and dissemination of scientific research documents, whether they are published or not. The documents may come from teaching and research institutions in France or abroad, or from public or private research centers.

L'archive ouverte pluridisciplinaire **HAL**, est destinée au dépôt et à la diffusion de documents scientifiques de niveau recherche, publiés ou non, émanant des établissements d'enseignement et de recherche français ou étrangers, des laboratoires publics ou privés.

Distributed under a Creative Commons CC BY-NC 4.0 - Attribution - Non-commercial use - International License

Check for updates

JGR Atmospheres

RESEARCH ARTICLE
10.1029/2025JD044219

Special Collection:
Advancements in Observing Atmospheric Composition from Hyperspectral Infrared Sensors

Post-Monsoon Pollution Events in the Indo-Gangetic Plain Using 18 Years [2007–2024] of IASI Carbon Monoxide Satellite Measurements

Selviga Sinnathamby[1], Sarah Safieddine[1], Marie Doutriaux-Boucher[2], Pierre Coheur[3], and Cathy Clerbaux[1,3]

[1]LATMOS/IPSL, Sorbonne Université, UVSQ, CNRS, Paris, France, [2]EUMETSAT, Darmstadt, Germany, [3]Spectroscopy, Quantum Chemistry and Atmospheric Remote Sensing (SQUARES), BLU-ULB Research Center, Université Libre de Bruxelles (ULB), Brussels, Belgium

Abstract In recent years, the Indo-Gangetic Plain (IGP) has experienced recurring intense air pollution episodes during the post-monsoon season (October–November), posing significant health risks to millions of inhabitants. These pollution events coincide with agricultural waste burning, emitting large quantities of carbon monoxide (CO) into the troposphere. Using 18 years of Infrared Atmospheric Sounding Interferometer (IASI) measurements from the Metop satellites, we examined the interannual variability of CO concentrations over the IGP during the post-monsoon season from 2007 to 2024. We focused on three representative years with varying CO levels (2011, 2017, and 2024) to determine whether CO pollution events in the IGP were more influenced by fire intensity, represented by the Fire Radiative Power (FRP) from the Moderate Resolution Imaging Spectroradiometers, or by meteorological parameters, particularly average winds in the 0–2 km layer, provided by ERA5 reanalysis. The comparison of wind patterns and FRP showed that surface winds primarily drive CO pollution severity. Extreme CO concentrations were found in 2017 and 2024 which coincided with prolonged periods of weak surface winds. In contrast, 2011 exhibited moderate CO concentrations throughout the post-monsoon season due to stronger winds, despite higher FRP. Our findings highlight the influence of surface winds in conditioning extreme post-monsoon pollution episodes in the IGP and demonstrate the ability of IASI for long-term monitoring of regional air pollution caused by agricultural waste burning. However, these results rely on the accurate detection of fire activity, which remains challenging due to limitations in satellite observations and changes in agricultural practices.

Plain Language Summary The burning of crop waste practiced every year in October and November negatively impacts air quality in the Indo-Gangetic Plain (IGP) as it releases many pollutants into the atmosphere, such as carbon monoxide (CO). In this study, we investigated how CO levels have changed from one year to another in the IGP region from 2007 to 2024, using satellite observations from the Infrared Atmospheric Sounding Interferometer (IASI). To understand whether CO levels are more driven by the intensity of crop waste burning or meteorological conditions, especially surface winds, we analyzed pollution events of 2011, 2017, and 2024, which exhibited different CO patterns in the region. We found that surface winds played a major role in shaping CO pollution. In 2017 and 2024, weak surface winds favored the buildup of CO, leading to extreme levels, while stronger winds in 2011 helped disperse CO across the region, resulting in lower levels despite high fire activity that year.

Key Points:

- Agricultural waste burning in the Indo-Gangetic Plain during post-monsoon can be monitored using carbon monoxide measurements from the Infrared Atmospheric Sounding Interferometer
- Abnormally high carbon monoxide levels were recorded during the post-monsoon season of 2017 and 2024, coinciding with weak surface winds
- Improved fire monitoring is needed to distinguish the influence of agricultural waste burning from meteorology during pollution events

Supporting Information:

Supporting Information may be found in the online version of this article.

Correspondence to:

S. Sinnathamby,
selviga.sinnathamby@latmos.ipsl.fr

Citation:

Sinnathamby, S., Safieddine, S., Doutriaux-Boucher, M., Coheur, P., & Clerbaux, C. (2026). Post-monsoon pollution events in the Indo-Gangetic Plain using 18 years [2007–2024] of IASI carbon monoxide satellite measurements. *Journal of Geophysical Research: Atmospheres*, *131*, e2025JD044219. https://doi.org/10.1029/2025JD044219

Received 5 MAY 2025
Accepted 15 DEC 2025

Author Contributions:

Conceptualization: Selviga Sinnathamby, Sarah Safieddine, Cathy Clerbaux
Formal analysis: Selviga Sinnathamby
Investigation: Selviga Sinnathamby
Supervision: Sarah Safieddine, Cathy Clerbaux
Visualization: Selviga Sinnathamby

© 2026 The Author(s).
This is an open access article under the terms of the Creative Commons Attribution-NonCommercial License, which permits use, distribution and reproduction in any medium, provided the original work is properly cited and is not used for commercial purposes.

1. Introduction

The Indo-Gangetic Plain (IGP) is a vast agricultural and industrial region, extending over multiple provinces in eastern Pakistan, states in northern India, and Bangladesh. It is delimited by the Hindu Kush and Himalayan mountain ranges on the west and the north, respectively. This region is highly populated, with more than 600 million inhabitants (~40% of the South Asian population) living there, despite only covering 20% of the subcontinent (Bangladesh Bureau of Statistics, 2022; Indian National Commission on Population, 2020; Pakistan Bureau of Statistics, 2023).

Over the past few decades, the IGP has experienced significant economic and industrial development, accompanied by a deterioration in regional air quality, as evidenced by high levels of pollutants, many of which serve as precursors to fine particulate matter ($PM_{2.5}$) (N. Singh et al., 2021). The region is home to a large number of coal-

Writing – original draft: Selviga Sinnathamby
Writing – review & editing: Sarah Safieddine, Marie Doutriaux-Boucher, Pierre Coheur, Cathy Clerbaux

fired thermal power plants, cement factories, large oil refineries, and other small to medium-scale industries (Chawala et al., 2023). In addition, the high population density in the region results in significant residential energy consumption that relies primarily on biofuel from coal, animal dung, and wood (Conibear et al., 2020; Pandey et al., 2017). Vehicle emissions also contribute to the degradation of the air quality (Bajwa & Sheikh, 2023; R. Singh et al., 2017), although the industrial and residential sectors remain the main sources of surface air pollution in the region, together accounting for more than half of the $PM_{2.5}$ emissions (Ghosh et al., 2024).

Another source of air pollution is the agricultural sector, a vital component of the economy of the IGP. Indeed, this region is often referred to as the agricultural heartland of South Asia, with its fertile lands irrigated by the Indus and the Ganges rivers and their tributaries. The region mainly grows rice, wheat, maize, sugarcane, and cotton, following an agricultural calendar typically consisting of two or three cropping cycles. Crop calendars are defined by the timing of the monsoon season, during which the land benefits from rainfall from June to September. This season is preceded by the winter (December to February) and the pre-monsoon seasons (March to May) and followed by the post-monsoon season (October and November).

In the northwestern Indian states of the IGP (Punjab, Haryana, and Uttar Pradesh), the dominant cropping cycle is the rice-wheat one (Wang et al., 2022): rice is planted in May and then harvested in October–November, while wheat is sown in November and then harvested in April–May. Eastern Pakistani provinces of the IGP (Sindh and Punjab) follow two other main cropping systems in addition to the rice-wheat one (mixed wheat and cotton-wheat) (Ahmad et al., 2015). This crop rotation system established during the Green Revolution in the early 1960s enables the northwestern Indian states of the IGP to be a major producer of wheat and rice in South Asia. They contribute approximately 22% of India's rice and 58% of its wheat production (Ministry of Agriculture and Farmers Welfare, Government of India, 2023). These crops generate significant amounts of residue (wheat stubble and rice straw), which can be managed in multiple ways, such as for cattle fodder or for industrial and domestic purposes (Parihar et al., 2023; Y. Singh & Sidhu, 2014). However, in practice, a large portion of crop residue is burned, particularly rice straw, because of its limited usability compared with wheat straw. It accounts for 60% of crop residues burned in India (Bhattacharyya et al., 2020). Multiple reasons lead farmers to open-field burning, including the fact that it is the most cost-effective option (Lopes et al., 2023). Another reason is the short time period between rice harvest and wheat planting, obliging farmers to quickly dispose of rice straw through burning (Ahmed et al., 2015). The sowing window has been further shortened in the Indian states of Haryana and Punjab following the implementation of the Preservation of Subsoil Water Acts in 2009, which aim to protect groundwater from overexploitation caused by intensive irrigation for rice cultivation. These laws require farmers to delay rice planting to align its growth period with the monsoon season, leading to higher fire activity in the post-monsoon season than the pre-monsoon season (Sembhi et al., 2020).

Agricultural waste burning has detrimental effects on regional air quality in the IGP, as it is a source of carbonaceous particles and several gaseous pollutants such as carbon monoxide (CO) (Sahu et al., 2021; K. P. Vadrevu et al., 2013). With a relatively long lifetime of one to 3 months (Holloway et al., 2000), CO is an excellent tracer of atmospheric pollution, capable of being transported over long distances and acting as a proxy for other pollutants simultaneously emitted by human activities and biomass burning (Badarinath et al., 2009; Roy et al., 2022). CO is a toxic gas produced during incomplete combustion processes but also through oxidation reactions of methane and non-methane hydrocarbons. It plays a crucial role in regulating the oxidative capacity of the troposphere, as its primary sink is the oxidation reaction with hydroxyl radicals (OH), which accounts for 40% of OH removal (Lelieveld et al., 2016).

During the post-monsoon season, CO levels rise due to the intensive burning of agricultural residues. Additionally, stable meteorological conditions typical of this season, such as temperature inversions and weak surface winds, contribute to the trapping of CO and other pollutants near the surface (Bilal et al., 2022; Kumari, Verma, et al., 2021). The combination of these factors leads to the formation of so-called “smog” events, which are generally characterized by hazardous $PM_{2.5}$ and CO concentrations and low visibility across the IGP (Goenka et al., 2024; Jethva et al., 2019; Majeed et al., 2024; Sawlani et al., 2019). These severe air pollution events have been studied extensively over the past decade because they pose a significant threat to the health of local populations (Lan et al., 2022) and to the climate, as the high load of absorbing aerosols perturbs the Earth's radiative budget (Choudhary et al., 2021).

21698996, 2026, 4, Downloaded from https://agupubs.onlinelibrary.wiley.com/doi/10.1029/2025JD044219 by Bibliothèque de Sorbonne Université, Wiley Online Library on [19/02/2026]. See the Terms and Conditions (https://onlinelibrary.wiley.com/terms-and-conditions) on Wiley Online Library for rules of use; OA articles are governed by the applicable Creative Commons License

21698996, 2026, 4, Downloaded from https://agupubs.onlinelibrary.wiley.com/doi/10.1029/2025JD044219 by Bibliothèque de Sorbonne Université, Wiley Online Library on [19/02/2026]. See the Terms and Conditions (https://onlinelibrary.wiley.com/terms-and-conditions) on Wiley Online Library for rules of use; OA articles are governed by the applicable Creative Commons License

The interest in post-monsoon pollution studies has been fueled by the proliferation of continuous air quality monitoring stations since 2015, in India in particular, providing daily measurements of a wide range of pollutants. However, these stations are mostly concentrated in urban areas (D. Sharma & Mauzerall, 2022). Satellite measurements offer a larger spatial coverage and can therefore be used to monitor the spatiotemporal variability of pollution events in the IGP. Several satellite instruments currently measure global daily CO concentrations, such as the Atmospheric Infrared Sounder (Aumann et al., 2003), the Measurements of Pollution in the Troposphere (MOPITT) instrument (Drummond et al., 2010), the Infrared Atmospheric Sounding Interferometer (IASI) (Clerbaux et al., 2009), the Cross-track Infrared Sounder (Han et al., 2013), and the TROPOspheric Monitoring Instrument (TROPOMI) (Veefkind et al., 2012).

In the present study, we investigate how CO concentrations have changed during the post-monsoon season in the IGP from 2007 to 2024, using the long data record of IASI measurements. We focus on identifying the key factors that determine the magnitude of post-monsoon CO concentrations as detected by IASI, from one year to another. We particularly want to determine whether they are more influenced by the intensity of the agricultural waste burning or by meteorological conditions, especially surface winds. To achieve this, we use, along the IASI CO data, Fire Radiative Power (FRP) data from the Moderate Resolution Imaging Spectroradiometer (MODIS), and ERA5 wind reanalysis, as described in Section 2. After presenting the climatology of CO, wind patterns, FRP for the post-monsoon season, and defining the areas of interest in Section 3.1, we discuss the interannual variability of CO levels during the post-monsoon season over the past 18 years in Section 3.2. In Section 3.3, we analyze selected pollution events to explain their differences in CO levels by examining the interplay between the agricultural waste burning intensity and the wind field patterns. Our conclusion and discussion are given in Section 4.

2. Data and Methods

2.1. IASI-Retrieved CO Concentrations

IASI is a space-borne Fourier Transform Spectrometer measuring the thermal infrared radiation emitted from Earth's surface and its atmosphere, in the 645–2760 cm^{-1} spectral range (Clerbaux et al., 2009). Three IASI instruments have been launched on board the sun-synchronous polar-orbiting meteorological satellites Metop-A (2006), -B (2012) and -C (2018). Metop-A has been in drifting orbit since mid-2019 and de-orbited in November 2021. The IASI mission has over 18 years of activity and is planned to last at least until 2034 with Metop-C. Each IASI instrument provides global coverage twice a day (09:30 a.m./p.m. local solar time) with a swath width of 2200 km. IASI observations are composed of 4 pixels with a circular footprint of 12 km diameter at nadir, elongating to an elliptical footprint of size 20 × 39 km at the end of the swath. Its high spectral resolution (0.5 cm^{-1}, apodized) allows columns and profile retrieval of a suite of diverse trace gases, such as CO (George et al., 2009), making it a high-performance instrument for monitoring atmospheric composition globally as well as extreme events, such as biomass fires (Turquety et al., 2009) and anthropogenic pollution (Boynard et al., 2013; Clarisse et al., 2011).

Near-real time (NRT) IASI CO total columns are retrieved using the Fast Optimal Retrieval on Layers for IASI algorithm (Hurtmans et al., 2012). This product has been validated against ground-based FTIR measurements (Kerzenmacher et al., 2012; Langerock, 2023), aircraft measurements (Barret et al., 2024), and other satellite observations (George et al., 2009). The European Organization for the Exploitation of Meteorological Satellites (EUMETSAT) has recently produced a homogeneous Climate Data Record (CDR) for CO (AC SAF, 2024a), using homogeneous IASI Metop-A and -B L1C radiances and consistent temperature profiles and cloud contamination flags. The CDR data set is available until December 2023 and can be completed with the NRT data set, as both are produced using the same retrieval algorithm (FORLIv20151001).

In this study, we averaged daily CO total columns using a combination of daytime and nighttime IASI data from different Metop platforms and from CDR and NRT products, as follows:

- 2007 to 2012: Metop-A (CDR)
- 2013 to 2019: Metop-A (CDR) + B (CDR)
- 2020 to 2023: Metop-B (CDR) + C (NRT)

In computing the average, it is also important to note that only the most reliable pixels, associated with a general quality flag value of 2 and cloud cover below 25%, were retained (AC SAF, 2024b). We also considered the most

21698996, 2026, 4, Downloaded from https://agupubs.onlinelibrary.wiley.com/doi/10.1029/2025JD044219 by Bibliothèque de Sorbonne Université, Wiley Online Library on [19/02/2026]. See the Terms and Conditions (https://onlinelibrary.wiley.com/terms-and-conditions) on Wiley Online Library for rules of use; OA articles are governed by the applicable Creative Commons License

sensitive pixels to the near surface in order to capture contribution from the surface during pollution events in the IGP. IASI shows a good sensitivity close to the surface in cases of large thermal contrast (TC), which is defined as the temperature difference between the surface and the first atmospheric layer just above. It has been shown that negative TC, where the temperature of the first atmospheric layer above the surface exceeds that of the surface (inversion layer), is often associated with higher sensitivity (Bauduin et al., 2017). Strong negative TC typically occurs over land at night during strong temperature inversions (Boynard et al., 2013), and some areas in the IGP frequently experience such conditions, facilitating the monitoring of high CO concentrations at night. As low CO total column error is associated with large TC when combined with high CO surface concentrations (Bauduin et al., 2017), we applied an error-based filter on both daytime and nighttime pixels: all pixels with an error above 7% of CO total column are discarded. This threshold value was considered after thorough examination of the error distribution over the IGP region and comparison with TROPOMI data, as described in Text S1 and Figures S1 and S2 in Supporting Information S1 (Borsdorff et al., 2018; Landgraf et al., 2016).

2.2. Fire Radiative Power From MODIS Terra and Aqua

To characterize the extent and intensity of agricultural waste burning in the IGP, we used FRP data, which is defined as the rate of fire energy released per unit time and is a key parameter commonly used to quantify the intensity of a fire. FRP is measured by the MODIS instruments, operating on the sun-synchronous polar-orbiting satellites Terra (since 2000) and Aqua (since 2002). Each MODIS instrument measures the radiation reflected and emitted by the Earth and its atmosphere in the visible and infrared range (from 0.4 to 14.4 μm) along a 2,300 km-wide swath. The two MODIS instruments cross the equator twice a day at approximately 10:30 a.m./p.m. (Terra) and 01:30 p.m./a.m. (Aqua) with a revisit time of 1–2 days.

FRP data at a spatial resolution of 1 km are taken from the MODIS/Aqua + Terra Thermal Anomalies/Fire locations 1 km V0061 product (MCD14DL, Giglio et al., 2016). For this study, we used daytime and nighttime data from both MODIS instruments, flagged with a confidence level ranging from 30% to 100% (nominal and high-confidence levels).

MODIS has difficulties in detecting fires that are smaller than its footprint (<1 km^2) or too cold, which can be often the case with crop residue burning fires (K. Vadrevu & Lasko, 2018). Other limitations arising from its scanning geometry, such as fires occurring between satellite overpasses, but also cloud and smoke obscuration, can lead to missed fires (Li et al., 2020). Despite these limitations, several fire trend studies in South Asia have been carried out in the past using MODIS fire products, showing that they are well-adapted to study agricultural waste burning (Liu et al., 2019; Potdar et al., 2024; Reddy et al., 2020; Sembhi et al., 2020; K. P. Vadrevu et al., 2013, 2019). Because MODIS provides consistent daily global fire observations over the entire 2007–2024 period, matching the temporal coverage of the IASI CO data set, we chose to use MODIS FRP data in this study. Note that the Visible Infrared Imaging Radiometer Suite (VIIRS) instrument has a better spatial resolution (375 m), but is not available for the entire studied period. Vadrevu and Lasko (2018) have demonstrated that MODIS effectively captures the main temporal dynamics of agricultural fires in Punjab, India, despite VIIRS detecting a greater number of fires and consequently reporting higher cumulative monthly FRP.

2.3. ERA5 Wind Reanalysis

We used daily horizontal winds as the main meteorological parameter to characterize pollutant transport across the IGP. Hourly 0.25 × 0.25° gridded horizontal u and v wind components at 37 pressure levels are provided by the fifth generation European Center for Medium-range Weather Forecast's (ECMWF) reanalysis (ERA5, Hersbach et al., 2020).

As ERA5 reanalysis is given in UTC hours, wind components were converted to Pakistan local time (UTC+05) beforehand and then averaged daily. We also average horizontal winds over pressure levels ranging from 1,000 hPa (∼surface) to 800 hPa (∼2 km), as CO emitted during agricultural waste burning is mainly contained in the boundary layer.

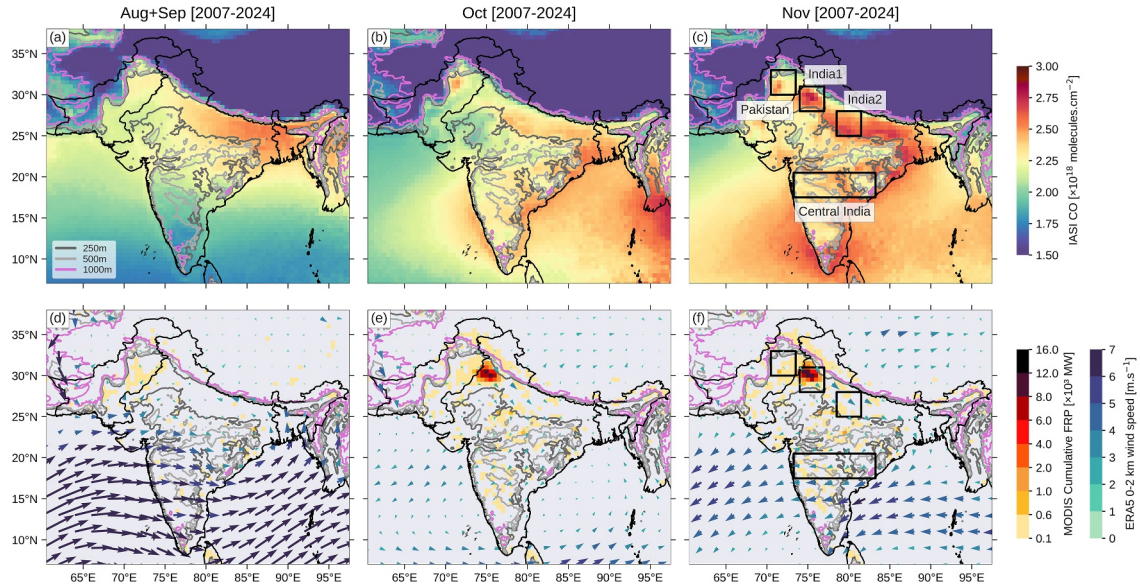

Figure 1. CO concentrations from IASI averaged over 2007–2024 for August and September combined (a), October (b), and November (c). Cumulative FRP from MODIS and ERA5 0–2 km winds averaged over 2007–2024 for August and September combined (d), October (e), and November (f). Altitude levels at 250, 500, and 1,000 m are outlined in dark gray, light gray, and pink, respectively. The areas of study are delimited by the black boxes in (c) and (f). FRP and CO data are gridded over a 0.5 × 0.5° grid.

3. Results

3.1. Post-Monsoon Climatology of CO, FRP, and Winds Over 2007–2024 and Areas of Study

Figure 1 shows the spatial distribution of CO concentrations, cumulative FRP and winds averaged over the 2007–2024 period for August and September combined (Figures 1a and 1d), October (Figures 1b and 1e), and November (Figures 1c and 1f). The combined climatology of August and September is used to represent the end of the monsoon season in South Asia, during which agricultural waste burning is not practiced in the IGP. Figure 1 highlights a clear difference in average CO concentrations between the end of the monsoon season and the post-monsoon season, with higher levels detected in November, particularly in the IGP, coinciding with the increase in FRP shown in the lower panels. The average winds, also shown in the lower panels of Figure 1, change between the end of the monsoon and the post-monsoon season. In central and southern India, they are generally strong (>6 $m.s^{-1}$) and blow from the Arabian Sea toward the Bay of Bengal at the end of the monsoon and then slow down and shift in the opposite direction during the post-monsoon season. In the IGP, winds remain very weak (<3 $m.s^{-1}$) from the end of the monsoon to the post-monsoon season, where they are south-easterly on average in the Indian parts of the IGP.

In the present work, we mainly examine three regions of size 3° × 3° within the IGP that we labeled as, from west to east, Pakistan, India1 and India2. We also define a 10° × 3° reference region located in central India, which is used as a reference for comparison with the IGP regions. All regions of study are outlined in black in Figures 1c and 1f. The Pakistan region is located in the province of Punjab in Pakistan, which is an agrarian province with the highest population density in the country (Pakistan Bureau of Statistics, 2023). The India1 region primarily includes the Indian states of Punjab and Haryana, where agricultural residue burning is intensively practiced. The India2 region is located within Uttar Pradesh, which is the most populated state in India and the IGP (Indian National Commission on Population, 2020). The Central India reference region encompasses vast areas of deciduous forests and agricultural fields (Reddy et al., 2020).

Figure 2 shows the daily time series of CO concentrations and cumulative FRP averaged over 2007–2024 for each of the regions of interest. A focus on FRP values for the India1 region is provided in Figure 2b, as its FRP values are significantly higher during the post-monsoon season, which is also visible in Figures 1e and 1f. We observe from Figure 2a that all three regions located in the IGP experience a rise in CO levels, with varying magnitudes, twice a year: from late April to May and from late October to early November.

21698996, 2026, 4, Downloaded from https://agupubs.onlinelibrary.wiley.com/doi/10.1029/2025JD044219 by Bibliothèque de Sorbonne Université, Wiley Online Library on [19/02/2026]. See the Terms and Conditions (https://onlinelibrary.wiley.com/terms-and-conditions) on Wiley Online Library for rules of use; OA articles are governed by the applicable Creative Commons License

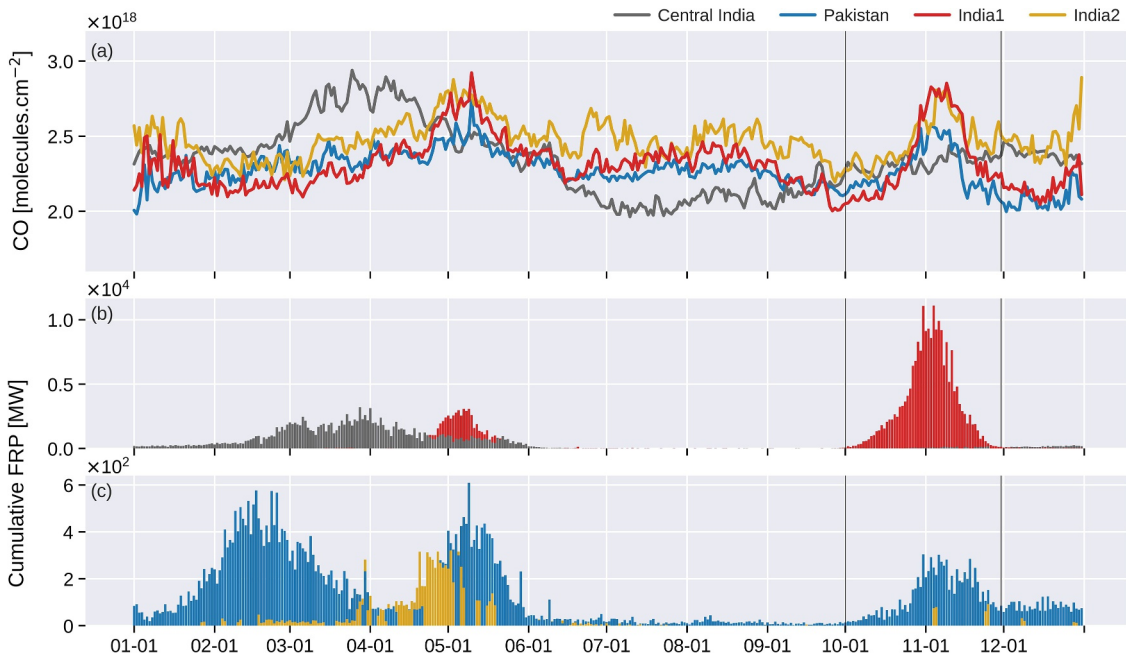

Figure 2. Daily time series of CO concentrations in (a) and cumulative FRP averaged over 2007–2024 separated for the India1 and Central India regions in (b) and the Pakistan and India2 regions in (c). Vertical black lines mark the post-monsoon season.

In the India1 region, these elevated CO periods coincide with increased fire activity linked to the intensive practice of crop residue burning by local farmers, as shown by the daily time series of FRP (Figure 2b). The maximum of fire activity in this region is found during the post-monsoon season and in particular between the end of October and the beginning of November. At this time of year, local winds are on average weak (~2 $m.s^{-1}$) and heading toward the southeast across the IGP, facilitating the transport of CO along the Himalayas (Figures 1e and 1f).

The India2 region, which is a downwind region with minor fire activity compared with the India1 region, also exhibits an increase in CO concentrations in early November (Figures 2a and 2c).

The region of Pakistan also experiences a rise in CO concentrations during the post-monsoon season, although it is less pronounced than in India1 and India2 regions (Figure 2a). Agriculture waste burning is also common in this region, although the cumulative FRP values averaged over 2007–2024 are significantly lower than in India1 (Figures 2b and 2c). This region experiences several periods of fire activity, coinciding with the harvest of different crops (sugar cane in December-February, wheat in April–May, and rice in October–November) (Azhar et al., 2019). However, fire activity is at its lowest on average in this region during the post-monsoon season. The rise in CO concentrations at this time of the year can be explained by the weak wind observed locally during the post-monsoon season (Figures 1e and 1f), favoring the buildup of CO, which can be originating from local fire and anthropogenic emissions. Some years, CO levels during the post-monsoon season can be influenced by agricultural waste burning practiced in India due to favoring transport pathways (Majeed et al., 2024).

Unlike the regions of interest located within the IGP, the Central India region (Figure 2a) exhibits a different daily pattern in CO concentrations. The daily time series of CO concentrations in this region is characterized by the typical seasonal cycle, with the highest levels observed around March–April due to reduced OH concentrations. CO levels reach their minimum during the monsoon season when winds are stronger compared with the IGP, where CO concentrations remain elevated (Figures 1d and 2a). From September onwards, CO levels increase as local winds weaken (Figures 1e, 1f, and 2a). Local fire activity, especially forest fires, can also contribute to elevated CO levels in March–April (Nirmalkar & Deb, 2016; Potdar et al., 2024). From Figure 2b, no fire activity is found during the post-monsoon season, generally resulting in lower CO concentrations compared to the regions of interest located in the IGP, making this area an ideal reference region for our study.

21698996, 2026, 4, Downloaded from https://agupubs.onlinelibrary.wiley.com/doi/10.1029/2025JD044219 by Bibliothèque de Sorbonne Université, Wiley Online Library on [19/02/2026]. See the Terms and Conditions (https://onlinelibrary.wiley.com/terms-and-conditions) on Wiley Online Library for rules of use; OA articles are governed by the applicable Creative Commons License

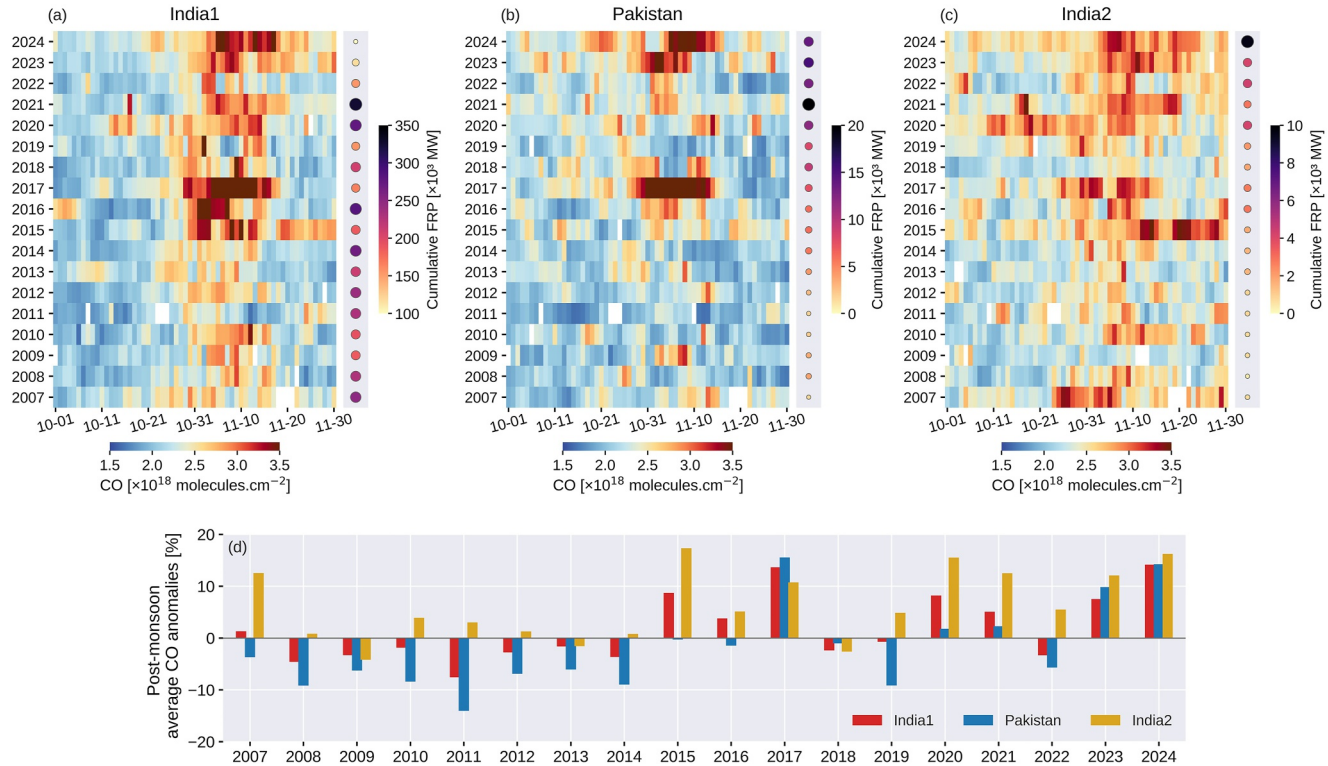

Figure 3. Upper panel: daily time series of CO concentrations during the post-monsoon season (October and November) from 2007 to 2024, averaged over India1 (a), Pakistan (b), and India2 (c) regions. Missing CO values are colored in white. Cumulative FRP over the post-monsoon seasons are indicated by colored circles on the right for each region. Lower panel (d): average CO anomalies (relative difference with respect to the Central India region) over the post-monsoon season for each region of interest.

3.2. Evolution of Post-Monsoon CO Concentrations and FRP From 2007 to 2024

In order to investigate the interannual variability of post-monsoon CO and FRP over the 2007–2024 period, we show in Figure 3 the daily time series of CO concentrations in the India1 (Figure 3a), Pakistan (Figure 3b), and India2 (Figure 3c) regions from 2007 to 2024. Missing values in the time series are typically due to the presence of clouds in the observation scene or occasional technical issues (18–21 November 2007, e.g.). Cumulative FRP over the post-monsoon season for each year are shown on the right for each region. The size and colors of the circles indicate the importance of fire activities within the region. Figure 3d shows the average CO anomalies during the post-monsoon seasons for each of the regions of interest within the IGP. Here, the daily anomalies are defined as the relative difference (in percent) between the daily CO concentrations in the region of interest and the daily climatology of the reference region, as described in Section 3.1. Since we only show the average anomaly value for the different post-monsoon seasons, a strong positive anomaly can result from either a few days of anomalous concentrations of CO ($>3.25 \times 10^{18}$ molecules.cm^{-2}) or from elevated CO values ($>2.5 \times 10^{18}$ molecules.cm^{-2}) lasting over a longer period (more than 3 weeks).

From Figure 3, we observe that daily CO concentrations vary from one region to another and from 1 year to another. In the India1 region, high CO concentrations typically occur between October 25 and November 15 over the 2007–2024 period (Figure 3a), aligning with the peak of fire activity in that region as mentioned in Section 3.1. Some years deviate from this pattern, with elevated CO concentrations detected as early as mid-October, such as in 2020, or persisting into late November, such as in 2015. The 2015 post-monsoon season was particularly distinct as it coincided with the Great Indonesian fires, releasing large amounts of CO that were transported to South Asia in the upper troposphere (Nandi et al., 2020). As CO concentrations in the IGP may have been affected by this extreme event, the 2015 post-monsoon season is not further considered in this study.

In contrast to the India1 region, identifying a clear pattern in daily CO concentrations over the 18 years is more challenging for the Pakistan and India2 regions. Days with high CO concentrations in the Pakistan region are less

21698996, 2026, 4, Downloaded from https://agupubs.onlinelibrary.wiley.com/doi/10.1029/2025JD044219 by Bibliothèque de Sorbonne Université, Wiley Online Library on [19/02/2026]. See the Terms and Conditions (https://onlinelibrary.wiley.com/terms-and-conditions) on Wiley Online Library for rules of use; OA articles are governed by the applicable Creative Commons License

21698996, 2026, 4, Downloaded from https://agupubs.onlinelibrary.wiley.com/doi/10.1029/2025JD044219 by Bibliothèque de Sorbonne Université, Wiley Online Library on [19/02/2026]. See the Terms and Conditions (https://onlinelibrary.wiley.com/terms-and-conditions) on Wiley Online Library for rules of use; OA articles are governed by the applicable Creative Commons License

frequent and more spread out across the post-monsoon seasons while India2 experiences longer periods of days with elevated CO levels (Figures 3b and 3c). This observation is also reflected in the average anomalies for the India2 region, which are predominantly positive, and for the Pakistan region, which are generally negative over the 18 years (Figure 3d).

However, some post-monsoon seasons in those regions exhibit similar features to those found in the India1 region, such as in 2017 or 2024. From Figures 3a and 3b, we observe anomalous CO concentrations ($>3.25 \times 10^{18}$ molecules.cm^{-2}) in Pakistan and India1 during the post-monsoon seasons of 2017 and 2024, lasting at least 12 days. These 2 years show the highest positive anomalies relative to the background region (>+12%) among the 18 years in the two regions (Figure 3d). Extreme CO concentrations are also observed in 2023 but only in the Pakistan region (Figure 3b). At the same time, the India1 region also experiences elevated CO concentrations, but not as high as those detected in Pakistan, explaining the higher average anomaly seen in the Pakistan region for that year (Figure 3d). We find a reverse phenomenon in 2016, when anomalous CO concentrations are detected in India1 for about a week but at a lower magnitude in Pakistan (Figures 3a and 3b). This explains the weak negative anomaly observed in Pakistan in 2016 while India1 experiences a weak positive anomaly (Figure 3d).

The 2016 and 2017 post-monsoon pollution events have been extensively studied due to the abnormally high $PM_{2.5}$ levels recorded at sites close to the burning areas (Chauhan & Singh, 2017; Kanawade et al., 2020; Mushtaq et al., 2024; Sawlani et al., 2019). These elevated $PM_{2.5}$ levels were generally associated with anomalous CO levels, which were measured by other satellite instruments such as MOPITT and TROPOMI (Dekker et al., 2019; Kanawade et al., 2020; Kumari, Lakhani, & Kumari, 2021). Although we find the most intense agricultural waste burning occurring in 2016, with a cumulative FRP of 282×10^3 MW (+36% above the 2007–2024 climatological mean of India1), extreme CO concentrations were observed over a shorter period than in 2017. In 2017, cumulative FRP was lower (166×10^3 MW, −21% relative to climatology), yet CO levels remained elevated for a longer duration (Figure 3a). Interestingly, the 2024 post-monsoon season recorded the lowest cumulative FRP in the India1 region over the 18-year period (54×10^3 MW, −74% anomaly), as shown in Figure 3a. The Pakistan and India2 regions show an increased local fire activity for that year, although it remains significantly lower than in India1 (Figures 3b and 3c). For the India2 region, even though CO concentrations are not as extreme as those measured in the India1 and Pakistan regions over the 2007–2024 period, the highest concentrations are generally detected around the same time, which is the case for the post-monsoon seasons of 2016, 2017, and 2024 (Figure 3c). This similarity can be attributed to India2 being downwind of India1 and experiencing much lower fire activity, as explained in Section 3.1.

Elevated CO concentrations are also found in 2020 and 2021 for several weeks in the India2 region, explaining the strong positive anomaly values found in this region during these years, especially in 2020, when it exceeds +15% (Figure 3d). Positive anomalies are also observed in the India1 and Pakistan regions, although they are significantly lower in Pakistan (<+5%). The post-monsoon seasons of 2020 and 2021 are particularly noticeable as they record the highest cumulative FRP values over the 2007–2024 period in the India1 region (277×10^3 MW, +33% anomaly and 326×10^3 MW, +57% anomaly, respectively), following a general decline in FRP between 2007 and 2019 (Figure 3a). This is likely due to labor shortages during the COVID-19 pandemic, as many workers returned to their home states, reducing workforce availability for crop residue management and possibly increasing paddy burning (Ravindra et al., 2022). Additionally, prolonged farmer protests in Punjab and Haryana against the Farm Acts introduced in 2020, which continued until the end of 2021, may have further intensified this practice (Mehta & Badegaonkar, 2023). It is noteworthy that elevated CO concentrations are recorded in the Pakistan region but only for a few days at the beginning of November 2021, even though this region experiences the highest fire activity recorded over the 2007–2024 period that year (24×10^3 MW, +287% above the 2007–2024 climatological mean of Pakistan), as shown in Figure 3b.

Some years have significantly lower CO concentrations, such as 2009, 2013, and 2018, where we find a negative anomaly in all three regions of interest, though the magnitude varies by region (Figure 3d). In general, the India2 region experiences very few years with negative anomalies, for the reasons explained above. When they do occur, these anomalies remain weak (<+5%), as it is the case for these three post-monsoon seasons. On the other hand, the India1 and Pakistan regions exhibit negative average anomalies for half of the post-monsoon seasons over the 18-year period. In particular, we notice that when the Pakistan region shows strong negative anomalies (<−5%), the India1 region also presents negative anomalies, although they are weaker in absolute value (>−5%). Only

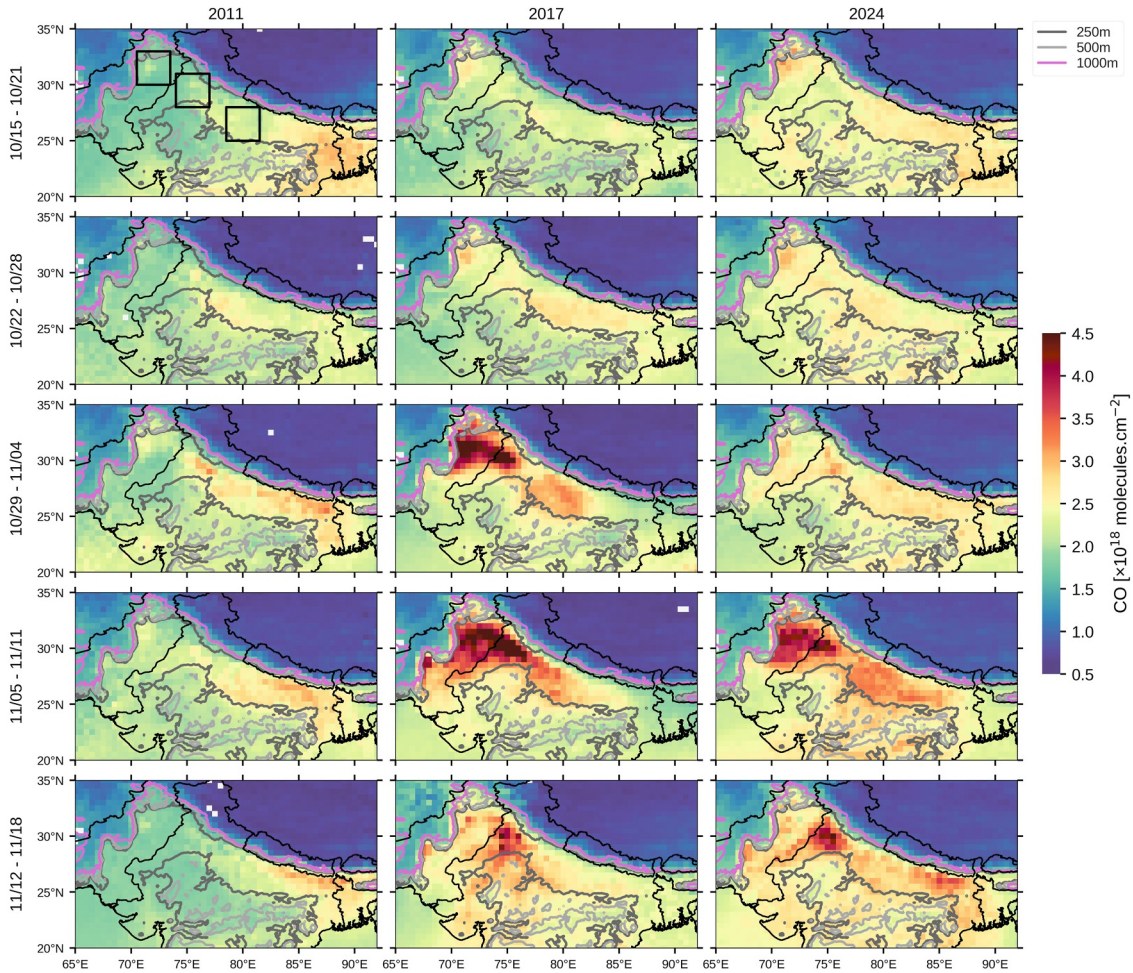

Figure 4. Maps of 7-day averaged CO concentrations from October 15 to November 18 (top to bottom) in 2011 (left), 2017 (middle), and 2024 (right). Altitude levels at 250, 500, and 1,000 m are outlined in dark gray, light gray, and pink, respectively. Regions of interest are indicated by the boxes on the uppermost left panel.

2011 stands out with particularly strong negative anomalies in both regions. This year records the most significant negative anomaly of the 18-year period, reaching −14% in Pakistan and −7% in India1. We note that 2011 is not associated with low fire activity in the India1 region (231×10^3 MW, +11% anomaly), as shown in Figure 3a.

To better understand the interannual and regional variations of CO, we select 2011, 2017, and 2024 as representative years to examine the factors influencing the intensity of CO pollution in each region as detected by IASI. These years are mainly chosen based on the observations made in the India1 region, where agricultural waste burning is most prevalent in the IGP. 2011 represents a case of low CO pollution (significant negative anomaly) and 2017, a case of strong CO pollution over several days. 2024 is included due to the significant positive anomaly observed that year, in addition to being the most recent and not yet studied post-monsoon pollution event.

3.3. Case Study of 2011, 2017, and 2024 Post-Monsoon Seasons: Impact of Winds and Agricultural Waste Burning on CO Levels

Figure 4 shows the 7-day averaged CO concentration maps from October 15 to November 18 for 2011, 2017, and 2024 while Figure 5 shows the cumulative FRP for the same period along with the corresponding 0–2 km wind direction and wind speed maps. To capture more clearly the day-to-day evolution of CO concentrations in relation to winds, we plotted the daily time series of average CO concentrations, cumulative FRP and average wind direction and speed for the India1, Pakistan, and India2 regions over the three selected years in Figures 6–8, respectively. Wind vectors are plotted as arrows, indicating the direction toward which the wind is blowing, while the color represents wind speed from yellow (0 $m.s^{-1}$) to purple (≥6 $m.s^{-1}$). For the FRP data, the assessment of

21698996, 2026, 4, Downloaded from https://agupubs.onlinelibrary.wiley.com/doi/10.1029/2025JD044219 by Bibliothèque de Sorbonne Université, Wiley Online Library on [19/02/2026]. See the Terms and Conditions (https://onlinelibrary.wiley.com/terms-and-conditions) on Wiley Online Library for rules of use; OA articles are governed by the applicable Creative Commons License

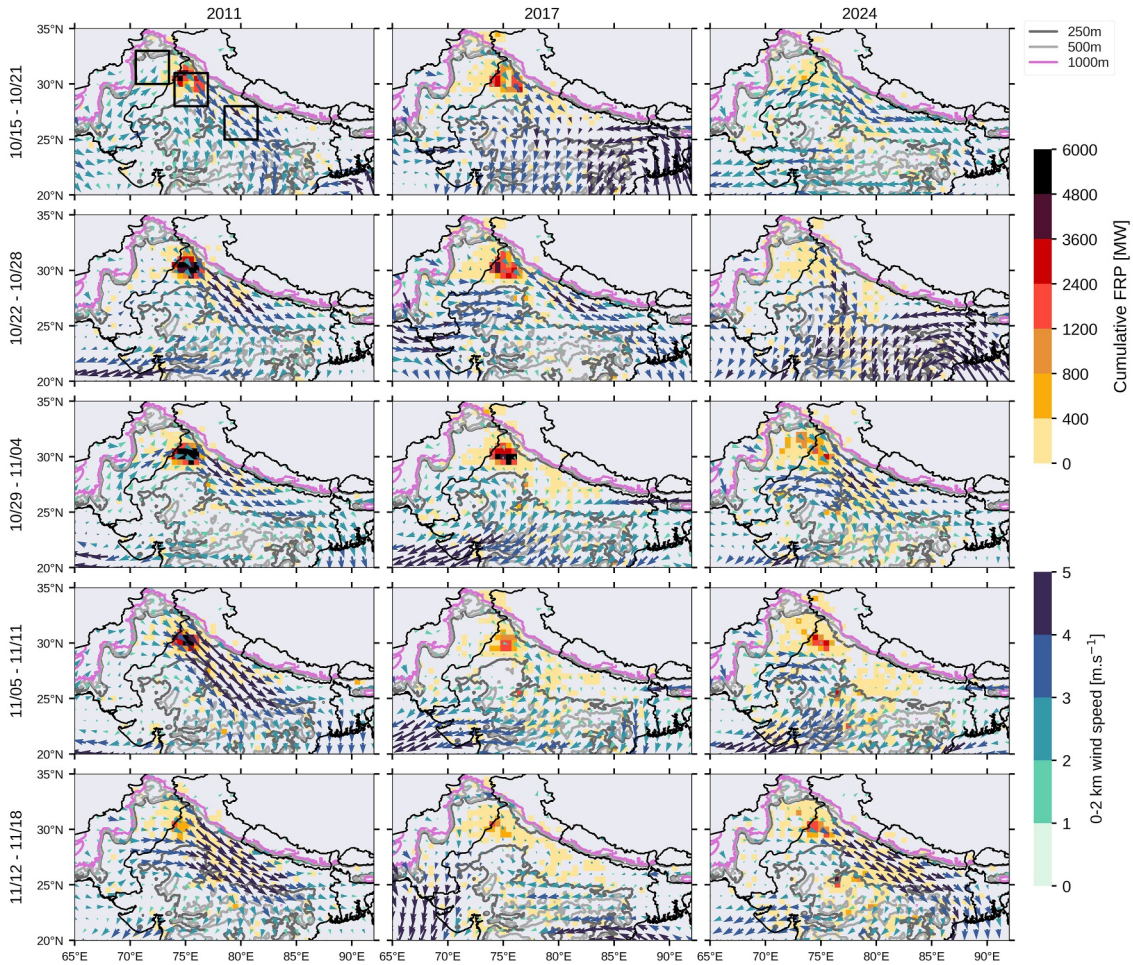

Figure 5. Maps of 7-day averaged 0–2 km wind direction and speed overlaid on 7-day cumulative FRP from October 15 to November 18 (top to bottom) in 2011 (left), 2017 (middle), and 2024 (right). FRP is shown from yellow (0 MW) to black (≥6,000 MW) while wind speed is represented from light blue (0 m.s^{-1}) to dark blue (≥5 m.s^{-1}). Altitude levels at 250, 500, and 1,000 m are outlined in dark gray, light gray, and pink, respectively. Regions of interest are indicated by the boxes on the uppermost left panel.

daily cloud pixel fractions as detected by MODIS (Aqua and Terra, day and night separated) for 2011, 2017, and 2024 shows that cloud contamination has minimal impact on FRP detection, as cloud pixel fraction exceeding 5% occurred on only a few days (less than a week) for each study region over the post-monsoon season (Figures S3, S4, and S5 in Supporting Information S1).

Pollution events generally develop under stable meteorological conditions, characterized by low precipitation, a shallow boundary layer, temperature inversion layer, and weak surface winds (Bilal et al., 2022; Garsa et al., 2023). We investigate surface winds in the section as the meteorological factor that would influence CO pollution events in the IGP. Several reasons justify this choice:

- The post-monsoon season is known to be drier relative to the monsoon season, with the IGP experiencing a low number of moderate rainfall days (between 5 and 10 days) (Pal et al., 2021). Moreover, CO is not removed by rain.
- No abnormally low boundary layer height (BLH) is observed during periods of high CO concentrations. In fact, by examining the daily mean BLH for each region of interest over the three selected years, we find that BLH varied very little from year to year across the three regions, as shown by the daily time series of BLH in Figure S6 in Supporting Information S1.
- Surface temperature is implicitly accounted for in our study as we retain only IASI pixels with a strong thermal contrast (TC), ensuring high sensitivity to surface. Negative thermal contrasts, associated with inversion

21698996, 2026, 4, Downloaded from https://agupubs.onlinelibrary.wiley.com/doi/10.1029/2025JD044219 by Bibliothèque de Sorbonne Université, Wiley Online Library on [19/02/2026]. See the Terms and Conditions (https://onlinelibrary.wiley.com/terms-and-conditions) on Wiley Online Library for rules of use; OA articles are governed by the applicable Creative Commons License

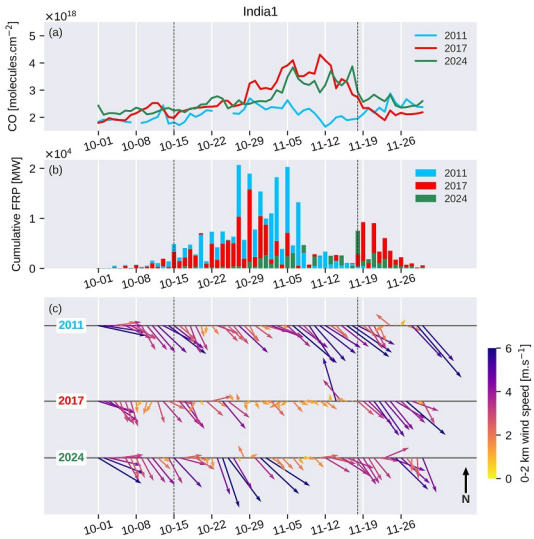

Figure 6. Daily time series of CO concentrations (a), cumulative FRP (b), and 0–2 km wind speed and direction (c) in the India1 region for the post-monsoon seasons of 2011, 2017, and 2024. The black arrow in the bottom right corner in panel (c) indicates a wind directed toward the North. Color scale indicates average wind speed values from yellow (0 m.s^{-1}) to purple (≥6 m.s^{-1}). The period from October 15 to November 18 is delimited by the dotted lines.

layers, are mostly observed in 2017 and 2024 but often during periods that do not necessarily coincide with those of elevated concentrations in the region of interest, as evidenced by the daily time series of thermal contrast (TC) for the three regions in Figure S7 in Supporting Information S1. For example, in the India1 region, negative TCs are observed in 2017, but only during the week of November 5–12, whereas high CO concentrations are detected as early as the week of October 29, when the average TC was positive but not significant (Figure S7a in Supporting Information S1).

- Post-monsoon pollution in the IGP is a transboundary and regional phenomenon. Winds are the only meteorological variable that can effectively characterize the transport of pollutants.

3.3.1. The Onset of the CO Pollution Episode (October 15–28)

During the period of October 15–28, CO levels remain relatively low across the IGP for the three years studied, as shown in Figure 4. Slightly higher average CO concentrations (yellow to orange shades) are observed in specific areas, such as northern Pakistan in 2017 and 2024 and eastern India and Bangladesh during the week of October 15–21 in 2011.

These two weeks also mark the early stages of agricultural waste burning activities, which are most prominent in 2011 and 2017, as shown in Figure 5. In 2024, very low values of FRP are observed, suggesting a delayed onset of agricultural residue burning that year. Average winds for the 3 years, also shown in Figure 5, exhibit the typical pattern of the post-monsoon season: weak winds in Pakistan and stronger winds directed toward the Bay of Bengal in the Indian part of the IGP.

These observations are further reflected in the daily evolution of CO, FRP, and winds for each region of interest (Figures 6–8). CO time series confirm these generally low CO levels while also revealing a daily variability in CO concentrations between the years and regions (Figures 6a, 7a and 8a). Changes in wind speed and direction can occasionally influence local CO concentrations, as in 2024 in the India1 region, where a noticeable reduction in wind speed starting on October 20 (from 6.6 m.s^{-1} on October 15 to 0.9 m.s^{-1} on October 20) lead to a small increase in CO (from 2.2 × 10^{18} to 2.5 × 10^{18} molecules.cm^{-2}), while winds predominantly blew toward the southeast during the 2 weeks (Figures 6a and 6c). In the India2 region, winds blow mainly toward the southeast and their speed is comparable to that observed in the India1 region, although some deviations toward other directions are also observed on certain days, such as southwest on 18 October 2017 (Figure 8c). The Pakistan region differs from the India1 and India2 regions in having consistently weak winds with variable directions over the 3 years examined (Figure 7c). Overall, for all 3 years, the wind fields found in Indian parts of the IGP promote effective air mass dispersion, preventing the accumulation of CO despite intense anthropogenic activities and agricultural waste burning.

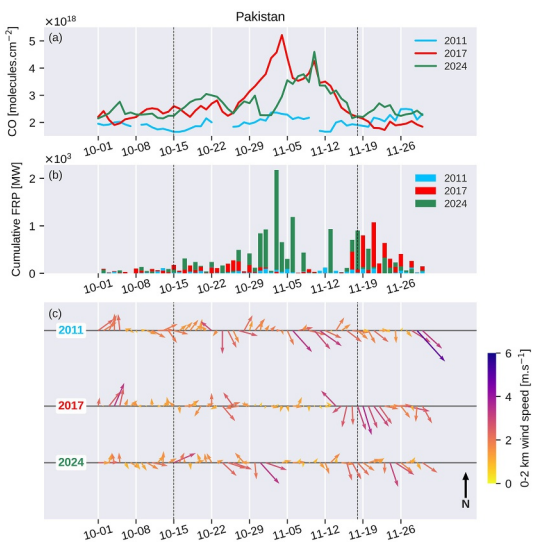

Figure 7. Same as Figure 6 but for the Pakistan region.

3.3.2. Rise and Persistence of CO Pollution (October 29–November 11)

The period from October 29 to November 11 is characterized by an increase in CO levels, marking the beginning of a pollution event in certain regions, particularly in 2017 and 2024 (Figure 4). In 2017, anomalously high CO concentrations are detected as early as the week from October 29 to November 4 across the IGP, then intensify and expand from the western to central parts of the IGP in the following week. A similar pattern in CO concentrations is observed in 2024, but it is limited to the week of November 5–11. In 2011, no anomalous CO concentrations are found, but central and eastern parts of the IGP still present elevated CO levels (Figure 4).

21698996, 2026, 4, Downloaded from https://agupubs.onlinelibrary.wiley.com/doi/10.1029/2025JD044219 by Bibliothèque de Sorbonne Université, Wiley Online Library on [19/02/2026]. See the Terms and Conditions (https://onlinelibrary.wiley.com/terms-and-conditions) on Wiley Online Library for rules of use; OA articles are governed by the applicable Creative Commons License

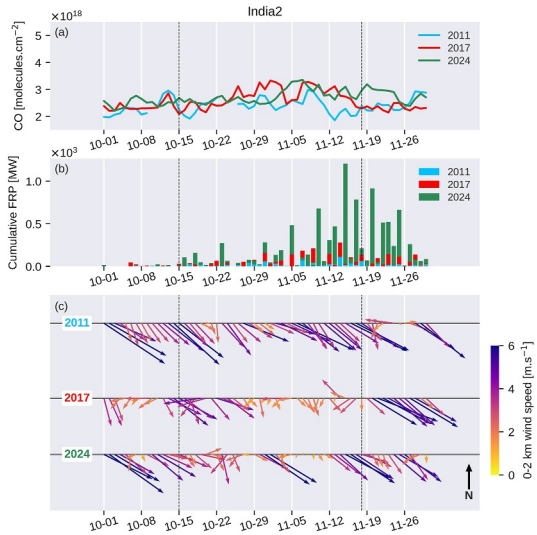

Figure 8. Same as Figure 6 but for the India2 region.

Figure 5 indicates that agricultural waste burning is most intense in 2011 throughout the two weeks. In 2017, it peaks between October 29 and November 4, whereas in 2024, it starts to rise during the same period but remains far less significant than in 2017 and 2011. Weak average winds prevail during the entire two-week period in 2017 and only from November 5–11 in 2024. In contrast, 2011 shows strong winds over the Indian IGP, blowing toward the Bay of Bengal throughout both weeks.

Anomalous CO levels are particularly noticeable in the India1 and Pakistan regions, with a sharp increase in daily CO concentrations over these two weeks in 2017 and 2024 (Figures 6a and 7a). In the India1 region, this rise occurs earlier in 2017 (October 29, with an average value of 3.2×10^{18} molecules.cm^{-2}) than in 2024 (November 5, 3.5×10^{18} molecules.cm^{-2}) (Figure 6a). The highest concentrations are observed in the Pakistan region for both years, and also occur later in 2024 (November 10, 4.6×10^{18} molecules.cm^{-2}) than in 2017 (November 4, 5.2×10^{18} molecules.cm^{-2}). Compared with 2017, CO levels in Pakistan are of the same magnitude for the week of November 5–11 (week average of 3.8×10^{18} molecules.cm^{-2} in 2017 and 3.7×10^{18} molecules.cm^{-2} in 2024), whereas they are lower in India1 in 2024 (3.8×10^{18} molecules.cm^{-2} in 2017 vs. 3.3×10^{18} molecules.cm^{-2} in 2024).

The difference in pollution intensity between 2017 and 2024 was also investigated by comparing IASI to surface measurements of $PM_{2.5}$ concentrations, which are provided by the U.S. State Department AirNow network and available from 2015 in New Delhi. The comparison is relevant since both CO and $PM_{2.5}$ are emitted by the same sources involving combustion processes. Daily time series of CO and $PM_{2.5}$ concentrations for 2017 and 2024 in New Delhi are shown in Figures S9a and S9b in Supporting Information S1. We find that CO and $PM_{2.5}$ concentrations are higher in 2017 than in 2024 in New Delhi, confirming IASI's ability to capture interannual pollution variability. The same comparison was also made for Lahore, but only for the 2024 pollution event (Text S2 and Figures S8, S9, and S10 in Supporting Information S1).

Over these two weeks, fire activity in the India1 region in 2017 decreases gradually after peaking on October 29, even though FRP values remain significantly higher than in 2024 with a cumulative FRP value of 79×10^3 MW in 2017 versus 25×10^3 MW in 2024 (Figure 6b). Interestingly, the Pakistan region experiences a sharp increase in fire activity in 2024, with FRP values exceeding those measured in 2011 and 2017 (6.1×10^3 MW in 2024 vs. 0.6×10^3 MW in 2017 and 0.5×10^3 MW in 2011) (Figure 7b). The maximum FRP value in Pakistan is reached on November 2, preceding the first CO peak (Figures 7a and 7b). The India2 region also shows a rise in fire activity in 2024, observed between October 30 and November 7 (2.2×10^3 MW in 2024 vs. 0.8×10^3 MW in 2017 and 0.3×10^3 MW in 2011), coinciding with an increase of CO for the same period (Figures 8a and 8b).

Although the intensity of the fires differs between these 2 years, both experience periods of very weak winds during these 2 weeks, but for different durations. In 2017, a marked change in wind direction and a reduction in wind speed are observed, particularly in India1 and India2, starting on October 26 and persisting until November 12 (Figures 6c and 8c). The coincidence of this shift in wind patterns and the important fire activity leads to a significant accumulation of CO across the IGP, including in the Pakistan region, where fire activity is considerably less intense than in the India1 region (Figure 7b). The smaller increase in CO concentrations observed in India2 can also be explained by the weak winds in India1 that restrict CO transport, in addition to modest local fire activity (Figures 6c and 8). We investigated the origin of the observed CO enhancement during this episode by performing a 3-day backward trajectory analysis using the HYSPLIT model (Stein et al., 2015) for 29 October 2017, which marks the onset of the sharp CO increase observed in the India1 and Pakistan regions (Figure S11 in Supporting Information S1). The results indicate that air masses reaching the India1 and Pakistan regions predominantly originated from fire-active areas in northwestern India and northeastern Pakistan. For the Pakistan region, 15 out of 27 trajectories (56%) originated from the India1 region while 6 extended from Pakistan toward India1 (Figures S11a and S11b in Supporting Information S1). In the India2 region, most trajectories came from eastern India, with a smaller fraction (25%) arriving from the India1 and Pakistan regions. Across all three regions, the trajectories remained confined within approximately 300 km, indicating stagnant atmospheric

21698996, 2026, 4, Downloaded from https://agupubs.onlinelibrary.wiley.com/doi/10.1029/2025JD044219 by Bibliothèque de Sorbonne Université, Wiley Online Library on [19/02/2026]. See the Terms and Conditions (https://onlinelibrary.wiley.com/terms-and-conditions) on Wiley Online Library for rules of use; OA articles are governed by the applicable Creative Commons License

21698996, 2026, 4, Downloaded from https://agupubs.onlinelibrary.wiley.com/doi/10.1029/2025JD044219 by Bibliothèque de Sorbonne Université, Wiley Online Library on [19/02/2026]. See the Terms and Conditions (https://onlinelibrary.wiley.com/terms-and-conditions) on Wiley Online Library for rules of use; OA articles are governed by the applicable Creative Commons License

conditions and limited long-range transport of CO. We also performed a backward trajectory analysis ending on 4 November 2017, corresponding to the maximum CO concentration recorded in the Pakistan region (Figure S12 in Supporting Information S1). The results show a similar dispersion pattern, with around 60% of trajectories intersecting fire-affected areas (i.e., pixels with non-zero FRP values during the 3-day simulation period), and about 25% originating from the India1 region, suggesting a contribution of local fires to the observed CO enhancements. Bilal et al. (2022) have documented this weak wind regime, attributing it to high-pressure anticyclonic systems extending from central Afghanistan to India, reinforced by an upper-level ridge at 500 hPa, which enhanced atmospheric subsidence and restricted surface-level CO dispersion. In 2024, a clear decline in wind strength is also observed for all three regions during this two-week period (Figures 6c, 7c, and 8c). From around November 3, winds shift from being relatively strong and directed toward the southeast to weaker and more variable directions, with mean speeds dropping between November 1 and 5 from 6.1 to 1.9 $m.s^{-1}$ in India1, from 2.8 to 0.9 $m.s^{-1}$ in Pakistan, and from 6.4 to 1.8 $m.s^{-1}$ in India2. These weak winds persist for approximately 8 days in the three regions, creating conditions that also lead to the accumulation of CO observed during the week of November 5–11. Backward trajectory analysis ending on 5 November 2024, was performed both to identify the potential source regions of the observed CO and to assess transport (Figure S13 in Supporting Information S1). For India1, most trajectories remained within the India1 region or extended approximately 200 km eastward, with a few originating from northern Pakistan at higher altitudes (Figure S13a in Supporting Information S1). In Pakistan, trajectories were predominantly linked to fire areas in India, with 16 out of 27 trajectories (∼60%) originating from the India1 region, and a smaller number linked to local sources, including 2 trajectories from southern Pakistan (Figure S13b in Supporting Information S1). For India2, most trajectories were clustered east of the region, all confined within a narrow corridor of ∼300 km in length (Figure S13c in Supporting Information S1). This confinement within a few hundred kilometers across all three regions highlights limited horizontal transport and persistent stagnation of air masses, which contributed to the CO accumulation observed during November 5–11.

Unlike 2017 and 2024, low CO levels are found in 2011 for all the regions of interest during the two weeks (Figures 6a, 7a, and 8a), confirming our observations made for Figure 4. These low concentrations are attributed to the strong winds blowing to the southeast, which have promoted continuous ventilation of air masses across the IGP, as evidenced by the wind time series for India1 and India2 (Figures 6c and 8c). Over this period, wind speeds in 2011 were significantly higher than in 2017 and 2024, with relative differences of −68% and −52% in India1 and India2, respectively, when comparing 2017 to 2011, and −48% and −39% when comparing 2024 to 2011. This flow also limits CO transport to the Pakistan region, which is minimally affected by fire activity, thereby explaining the low CO concentrations measured there as well (Figure 7). However, occasional decreases in wind speed in the India1 and India2 regions on certain days may have allowed for slight CO accumulation (Figures 6c and 8c), as this period still coincides with the peak of fire activity in the India1 region. Figure 6b confirms that fire activity during this period is significantly higher than in 2017 and 2024.

3.3.3. Decrease of CO From November 12 to 18: The End of the Pollution Event

The week of November 12–18 is characterized by a general decrease in CO levels across nearly the entire IGP, which is particularly noticeable in 2017 and 2024 (Figure 4). In 2011, CO concentrations remain low over the whole 5 weeks. This is explained by the stronger winds that continued to blow toward the southeast (Figure 5), especially in the India1 and India2 regions where average wind speeds reached 4.3 $m.s^{-1}$ and 5.2 $m.s^{-1}$, respectively (Figures 6c and 8c). The drop in FRP values in the India1 region also shows that this week marks the end of agricultural waste burning with a cumulative FRP of 8.5×10^3 MW compared with 44.2×10^3 MW for the previous week (Figure 6b).

In 2017, a reduction in CO levels is observed in the IGP while it remains elevated and appears to extend further south within the IGP, reaching as far as central India (Figure 4). Simultaneously, a drop in FRP values is also observed during this week, particularly in the India1 region where the cumulative FRP dropped to 6.5×10^3 MW compared with 14.5×10^3 MW for the previous week (Figures 5 and 6c). Winds play a role in the transport and local reduction of CO pollution. While the average wind patterns indicate weak or negligible speeds across most of the IGP during the study period (Figure 5), daily time series reveal a notable increase in wind speed around November 13–14 in the regions of interest (Figures 6a, 6c, 7a, 7c, 8a, and 8c). For example, in India1, wind speeds reached 5.4 $m.s^{-1}$ on November 14, compared with a weekly average of 2.4 $m.s^{-1}$. Despite the wind direction toward the northwest in India1, which is generally unfavorable for CO dispersion, the relatively high wind speeds

21698996, 2026, 4, Downloaded from https://agupubs.onlinelibrary.wiley.com/doi/10.1029/2025JD044219 by Bibliothèque de Sorbonne Université, Wiley Online Library on [19/02/2026]. See the Terms and Conditions (https://onlinelibrary.wiley.com/terms-and-conditions) on Wiley Online Library for rules of use; OA articles are governed by the applicable Creative Commons License

enhanced ventilation by promoting the export of air masses out of the region, explaining the partial decrease in CO concentrations observed for those days. For the India1 region, winds regain their typical direction toward the southeast from November 18 onward with wind speeds increasing from 0.9 $m.s^{-1}$ on November 17 to 3.4 $m.s^{-1}$ on November 19, further promoting the dispersion of CO, whose concentration decreased from 2.74×10^{18} molecules.cm^{-2} on November 17 to 2.34×10^{18} molecules.cm^{-2} on November 19. In the Pakistan and India2 regions, daily wind speeds also increase compared with the period from October 29 to November 12 (Figures 7c and 8c). These stronger winds, with variable directions, particularly toward central India from the Pakistan region, can explain the broader and variable spatial distribution of CO observed in Figure 4.

As in 2017, 2024 experiences a general decline in CO levels across the IGP but elevated CO concentrations still persist in the northwestern parts of India (Figure 4). At the same time, average winds resume their usual post-monsoon pattern and fire activity is low all over the IGP (Figure 5). In fact, daily CO concentrations in India1 remain high for most of the week with an average value of 3.4×10^{18} molecules.cm^{-2} (similar to the previous week), before decreasing after November 17 (Figure 6a). The low daily FRP values observed in this region during that week suggest that agricultural waste burning activity is less prevalent this year, despite a peak in FRP on November 18 (Figure 6b). Meanwhile, wind speeds increase from November 12 onward (with a week average of 3.3 $m.s^{-1}$ vs. 1.5 $m.s^{-1}$ for the previous week) and are predominantly directed toward the southeast for most of the week (Figure 6c), which does not necessarily explain the high CO levels detected in the region. The elevated CO levels recorded in India1 during the week may have originated from Pakistan, where CO accumulated. From November 12, winds blowing toward the southeast in the Pakistan region likely transported this pollution to India1, although their speed was relatively low (Figure 7c). This is supported by HYSPLIT backward trajectories ending on November 15, selected as a representative day within the week, which indicate that most air masses arriving at India1 originated from Pakistan (17 out of 27 trajectories, ~63%) as well as from local fire hotspots (Figure S14a in Supporting Information S1). These winds also explain the decrease in CO levels observed in the Pakistan region during the same week (week average value of 2.79×10^{18} molecules.cm^{-2} vs. 3.7×10^{18} molecules.cm^{-2} for the previous week), despite ongoing fire activity, which is slightly less intense than in previous days (Figures 7a and 7b). In the India2 region, CO levels remain similar to those of the previous week, likely due to CO transport from the India1 region, where strong winds directed toward the southeast were observed during this period (Figure 8a). Backward trajectories calculated with HYSPLIT ending on November 15 support this, showing air masses arriving predominantly from the India1 region (13 out of 27 trajectories, 48%) and by nearby local fire hotspots (Figure S14b in Supporting Information S1). Indeed, while fire activity in India2 is significantly higher than in 2011 and 2017, it does not appear to have a substantial impact on local CO levels, as they are comparable to those years (Figure 8b). This limited impact can be attributed to the much higher wind speeds recorded in the India2 region during November 12–18, favoring CO dispersion toward the southeast (Figure 8c).

4. Conclusion and Discussion

The IGP suffers from recurrent intense pollution episodes during the post monsoon season. This study has examined CO levels in the region during this period, as observed by the IASI remote sensor over the period 2007–2024. This analysis of 18 years of data revealed that CO concentrations vary considerably from one year to another, with some years standing out for having exceptionally high concentrations recorded between late October and mid-November. This period coincides with the intensive practice of agricultural waste burning in the northwestern Indian states of the IGP.

By taking three representative years of different pollution cases (2011, 2017, and 2024), we analyzed the main factors behind these pollution episodes and tried to explain their differences in intensity, particularly by looking at the interactions between CO concentrations, the intensity of fire activity represented by FRP and average winds in the 0–2 km layer. The study of these three events revealed that the intensity of fires, as detected by MODIS, was not the only factor driving the magnitude of CO concentrations. In some cases, high FRP values did not translate into high CO levels, as in 2011, while in other cases, such as 2024, elevated CO occurred despite relatively low FRP. This indicates that extreme post-monsoon CO pollution episodes result from a combination of factors, with meteorological conditions, particularly stagnant surface winds, playing a predominant role. For instance, in both 2017 and 2024, prolonged periods of exceptionally low surface winds coincided with unusually high CO concentrations, regardless of the level of fire activity. Other meteorological parameters, such as BLH and temperature, were also examined, but they were found to have a much lower impact than surface winds.

21698996, 2026, 4, Downloaded from https://agupubs.onlinelibrary.wiley.com/doi/10.1029/2025JD044219 by Bibliothèque de Sorbonne Université, Wiley Online Library on [19/02/2026]. See the Terms and Conditions (https://onlinelibrary.wiley.com/terms-and-conditions) on Wiley Online Library for rules of use; OA articles are governed by the applicable Creative Commons License

The northwestern Indian states of the IGP are often pointed out as the main contributors to these extreme CO pollution episodes in the region. However, it is important to note that the IGP is already a heavily polluted region due to local emissions associated with intense anthropogenic activities. Agricultural waste burning further contributes to this already elevated background pollution, leading to extreme CO levels during the post-monsoon season, with contributions varying across the region (Dekker et al., 2019; A. Sharma et al., 2024). Reducing agricultural waste burning is therefore an essential first step in improving air quality in the IGP. Since 2016, a general decrease in fire activity detected by MODIS has been observed in the northwestern Indian states, suggesting a reduction of agricultural burning linked to improved local residue management, as rice crop areas have also continued to expand, notably in Punjab and Haryana, with increases of 23% and 50% between 2002 and 2022, respectively (Research Institute for Humanity and Nature, 2025). This improvement in residue management likely stems from government efforts, including machinery subsidies introduced in 2018 and the promotion of short-duration rice varieties since the early 2010s. These varieties generate less residue and provide a longer time gap between rice harvest and wheat sowing, giving farmers time to manage residues without burning (Kemanth et al., 2024). This decline in detected fire activity contrasts with the intensification of post-monsoon CO pollution events in recent years, highlighting the complexity of the situation. Meteorological conditions clearly influence extreme pollution episodes in the IGP but uncertainties remain due to potential underestimation of fires caused by MODIS' lower spatial resolution, smoke obscuration or changes in agricultural practices, such as the burning of crop residues outside the overpass times of NASA satellites (Pati, 2024), making it difficult to determine the relative importance of fire activity versus meteorology. These limitations highlight the need of geostationary satellites to provide hourly fire monitoring over long periods to better understand changes in burning practices and their impact on atmospheric composition.

Finally, this study shows that IASI is a suitable instrument for sounding pollution from agricultural waste burning. It is also one of the few studies to use nighttime IASI data, which are often discarded due to a potential lack of sensitivity near the surface. The combination of observations from the different IASI instruments allowed us to study these recurrent pollution events over a period of 18 years, providing a long-term assessment of the evolution of CO concentrations during the post-monsoon season. The continuity of the IASI mission is ensured by the IASI-New Generation mission, which will keep monitoring post-monsoon pollution events for at least 15 more years, with improved spectral resolution, allowing for more precise detection of CO in the lower troposphere.

Conflict of Interest

The authors declare no conflicts of interest relevant to this study.

Data Availability Statement

The IASI L2 Carbon Monoxide (CO) Climate Data Record (CDR) product is available on the EUMETSAT Data Store (https://user.eumetsat.int/catalogue/EO:EUM:DAT:0959, AC SAF, 2024a). Daily files generated from the CO-CDR orbit files can be downloaded from the Aeris portal (http://iasi.aeris-data.fr/CO/), as well as the IASI L2 Carbon Monoxide NRT from Metop-B (https://doi.org/10.25326/64) and Metop-C (https://doi.org/10.25326/65, last accessed on 19 December 2024).

The MODIS/Aqua + Terra Thermal Anomalies/Fire locations 1 km V0061 product (MCD14DL) is distributed by the FIRMS operated by NASA's Earth Science Data and Information System Project (https://doi.org/10.5067/FIRMS/MODIS/MCD14DL.NRT.0061, NASA MODIS Science Data Support Team, 2021, accessed on 2 March 2025).

Hourly ERA5 winds reanalysis on pressure levels are produced by the Copernicus Climate Change Service (C3S) at ECMWF and is distributed via the Copernicus Climate Data Store (https://doi.org/10.24381/cds.bd0915c6, Hersbach et al., 2023, accessed on 20 December 2024).

The Sentinel-5P TROPOMI L2 Carbon Monoxide Column product can be downloaded from NASA Goddard Earth Sciences Data and Information Services Center (GES DISC) website (https://doi.org/10.5270/S5P-bj3nry0, Copernicus Sentinel-5P (processed by ESA), Koninklijk Nederlands Meteorologisch Instituut (KNMI), and Netherlands Institute for Space Research (SRON), 2021, accessed on 10 February 2024).

$PM_{2.5}$ concentrations are provided by the U.S. State Department AirNow network (https://www.airnow.gov/, last accessed on 30 January 2025).

Acknowledgments
IASI is a joint mission of EUMETSAT and the Centre National d'Etudes Spatiales (CNES, France). We acknowledge the AERIS data infrastructure for providing access to the IASI data in this study and ULB-LATMOS for the development of the retrieval algorithms. We thank EUMETSAT through the Satellite Application Facility on Atmospheric Composition Monitoring (ACSAF) for the distribution of the IASI-CO product. We thank NASA's Fire Information for Resource Management System (FIRMS), part of NASA's Earth Observing System Data and Information System (EOSDIS) and the Copernicus Climate Data Store for providing MODIS and ERA5 data. We thank the team that realized the TROPOMI instrument and its data products, consisting of the partnership between Airbus Defence and Space Netherlands, KNMI, SRON, and TNO, commissioned by NSO and ESA. Sentinel-5 Precursor is part of the EU Copernicus program and Copernicus Sentinel-5P data (2023) have been used. We acknowledge the U.S. State Department for providing $PM_{2.5}$ concentrations.

References

AC SAF. (2024a). IASI carbon monoxide profiles FORLI-CO climate data record release 1—Metop-A and -B [Dataset]. *IASI carbon monoxide profiles FORLI-CO climate data record release 1—Metop-A and -B*. https://doi.org/10.15770/EUM_SAF_AC_0047

AC SAF. (2024b). IASI reprocessed L2 CO CDR (O3M-517) Metop-A and B product user manual. Tech. Rep. 1.3. *EUMETSAT*. Retrieved from https://user.eumetsat.int/catalogue/EO:EUM:DAT:0959

Ahmad, A., Ashfaq, M., Rasul, G., Wajid, S. A., Khaliq, T., Rasul, F., et al. (2015). Impact of climate change on the rice–wheat cropping system of Pakistan. In C. Rosenzweig & D. Hillel (Eds.), *ICP series on climate change impacts, adaptation, and mitigation* (Vol. 4, pp. 219–258). IMPERIAL COLLEGE PRESS. https://doi.org/10.1142/9781783265640_0019

Ahmed, T., Ahmad, B., & Ahmad, W. (2015). Why do farmers burn rice residue? Examining farmers' choices in Punjab, Pakistan. *Land Use Policy*, *47*, 448–458. https://doi.org/10.1016/j.landusepol.2015.05.004

Aumann, H. H., Chahine, M. T., Gautier, C., Goldberg, M. D., Kalnay, E., McMillin, L. M., et al. (2003). AIRS/AMSU/HSB on the Aqua mission: Design, science objectives, data products, and processing systems. *IEEE Transactions on Geoscience and Remote Sensing*, *41*(2), 253–264. https://doi.org/10.1109/TGRS.2002.808356

Azhar, R., Zeeshan, M., & Fatima, K. (2019). Crop residue open field burning in Pakistan; multi-year high spatial resolution emission inventory for 2000–2014. *Atmospheric Environment*, *208*, 20–33. https://doi.org/10.1016/j.atmosenv.2019.03.031

Badarinath, K. V. S., Kharol, S. K., Sharma, A. R., & Krishna Prasad, V. (2009). Analysis of aerosol and carbon monoxide characteristics over Arabian Sea during crop residue burning period in the Indo-Gangetic Plains using multi-satellite remote sensing datasets. *Journal of Atmospheric and Solar-Terrestrial Physics*, *71*(12), 1267–1276. https://doi.org/10.1016/j.jastp.2009.04.004

Bajwa, A. U., & Sheikh, H. A. (2023). Contribution of road transport to Pakistan's air pollution in the urban environment. *Air*, *1*(4), 237–257. Article 4. https://doi.org/10.3390/air1040018

Bangladesh Bureau of Statistics. (2022). *Population and Housing Census [Tech. Rep.]*. Statistics and Informatics Division, Ministry of Planning, Government of the People's Republic of Bangladesh.

Barret, B., Loicq, P., Le Flochmoën, E., Bennouna, Y., Hadji-Lazaro, J., Hurtmans, D., & Sauvage, B. (2024). Validation of 12 years (2008–2019) of IASI-CO with IAGOS aircraft observations. *EGUsphere*, 1–29. https://doi.org/10.5194/egusphere-2024-30

Bauduin, S., Clarisse, L., Theunissen, M., George, M., Hurtmans, D., Clerbaux, C., & Coheur, P.-F. (2017). IASI's sensitivity to near-surface carbon monoxide (CO): Theoretical analyses and retrievals on test cases. *Journal of Quantitative Spectroscopy and Radiative Transfer*, *189*, 428–440. https://doi.org/10.1016/j.jqsrt.2016.12.022

Bhattacharyya, P., Bhaduri, D., Adak, T., Munda, S., Satapathy, B. S., Dash, P. K., et al. (2020). Characterization of rice straw from major cultivars for best alternative industrial uses to cutoff the menace of straw burning. *Industrial Crops and Products*, *143*, 111919. https://doi.org/10.1016/j.indcrop.2019.111919

Bilal, M., Hassan, M., Tahir, D. B. T., Iqbal, M. S., & Shahid, I. (2022). Understanding the role of atmospheric circulations and dispersion of air pollution associated with extreme smog events over South Asian megacity. *Environmental Monitoring and Assessment*, *194*(2), 82. https://doi.org/10.1007/s10661-021-09674-y

Borsdorff, T., aan de Brugh, J., Hu, H., Hasekamp, O., Sussmann, R., Rettinger, M., et al. (2018). Mapping carbon monoxide pollution from space down to city scales with daily global coverage. *Atmospheric Measurement Techniques*, *11*(10), 5507–5518. https://doi.org/10.5194/amt-11-5507-2018

Boynard, A., Clerbaux, C., Clarisse, L., Safieddine, S., Pommier, M., Van Damme, M., et al. (2013). First simultaneous space measurements of atmospheric pollutants in the boundary layer from IASI: A case study in the North China Plain—Boynard—2014—Geophysical Research Letters—Wiley Online Library. *Geophysical Research Letters*, *41*(2), 645–651. https://doi.org/10.1002/2013GL058333

Chauhan, A., & Singh, R. P. (2017). Poor air quality and dense haze/smog during 2016 in the indo-gangetic plains associated with the crop residue burning and diwali festival. *2017 IEEE International Geoscience and Remote Sensing Symposium (IGARSS)*, 6048–6051. https://doi.org/10.1109/IGARSS.2017.8128389

Chawala, P., Priyan R, S., & Nagendra, S. M. (2023). Climatology and landscape determinants of AOD, SO2 and NO2 over Indo-Gangetic Plain. *Environmental Research*, *220*, 115125. https://doi.org/10.1016/j.envres.2022.115125

Choudhary, V., Singh, G. K., Gupta, T., & Paul, D. (2021). Absorption and radiative characteristics of brown carbon aerosols during crop residue burning in the source region of Indo-Gangetic Plain. *Atmospheric Research*, *249*, 105285. https://doi.org/10.1016/j.atmosres.2020.105285

Clarisse, L., R'Honi, Y., Coheur, P.-F., Hurtmans, D., & Clerbaux, C. (2011). Thermal infrared nadir observations of 24 atmospheric gases. *Geophysical Research Letters*, *38*(10), L10802. https://doi.org/10.1029/2011GL047271

Clerbaux, C., Boynard, A., Clarisse, L., George, M., Hadji-Lazaro, J., Herbin, H., et al. (2009). Monitoring of atmospheric composition using the thermal infrared IASI/MetOp sounder. *Atmospheric Chemistry and Physics*, *9*(16), 6041–6054. https://doi.org/10.5194/acp-9-6041-2009

Conibear, L., Butt, E. W., Knote, C., Lam, N. L., Arnold, S. R., Tibrewal, K., et al. (2020). A complete transition to clean household energy can save one–quarter of the healthy life lost to particulate matter pollution exposure in India. *Environmental Research Letters*, *15*(9), 094096. https://doi.org/10.1088/1748-9326/ab8e8a

Copernicus Sentinel-5P (processed by ESA), Koninklijk Nederlands Meteorologisch Instituut (KNMI), and Netherlands Institute for Space Research (SRON). (2021). Sentinel-5P TROPOMI Carbon Monoxide CO Column 1-Orbit L2 5.5km x 7km [Dataset]. *Goddard Earth Sciences Data and Information Services Center (GES DISC)*. https://doi.org/10.5270/S5P-bj3nry0

Dekker, I. N., Houweling, S., Pandey, S., Krol, M., Röckmann, T., Borsdorff, T., et al. (2019). What caused the extreme CO concentrations during the 2017 high-pollution episode in India? *Atmospheric Chemistry and Physics*, *19*(6), 3433–3445. https://doi.org/10.5194/acp-19-3433-2019

Drummond, J. R., Zou, J., Nichitiu, F., Kar, J., Deschambaut, R., & Hackett, J. (2010). A review of 9-year performance and operation of the MOPITT instrument. *Advances in Space Research*, *45*(6), 760–774. https://doi.org/10.1016/j.asr.2009.11.019

Garsa, K., Khan, A. A., Jindal, P., Middey, A., Luqman, N., Mohanty, H., & Tiwari, S. (2023). Assessment of meteorological parameters on air pollution variability over Delhi. *Environmental Monitoring and Assessment*, *195*(11), 1315. https://doi.org/10.1007/s10661-023-11922-2

George, M., Clerbaux, C., Hurtmans, D., Turquety, S., Coheur, P.-F., Pommier, M., et al. (2009). Carbon monoxide distributions from the IASI/METOP mission: Evaluation with other space-borne remote sensors. *Atmospheric Chemistry and Physics*, *9*(21), 8317–8330. https://doi.org/10.5194/acp-9-8317-2009

21698996, 2026, 4, Downloaded from https://agupubs.onlinelibrary.wiley.com/doi/10.1029/2025JD044219 by Bibliothèque de Sorbonne Université, Wiley Online Library on [19/02/2026]. See the Terms and Conditions (https://onlinelibrary.wiley.com/terms-and-conditions) on Wiley Online Library for rules of use; OA articles are governed by the applicable Creative Commons License

Ghosh, A., Nagar, P. K., Maddhesia, J., Sharma, M., Azmi, S., Singh, B., & Dutta, M. (2024). A district-level emission inventory of anthropogenic PM2.5 from the primary sources over the Indian Indo Gangetic Plain: Identification of the emission hotspots. *Science of The Total Environment*, *914*, 169865. https://doi.org/10.1016/j.scitotenv.2023.169865

Giglio, L., Schroeder, W., & Justice, C. O. (2016). The collection 6 MODIS active fire detection algorithm and fire products. *Remote Sensing of Environment*, *178*, 31–41. https://doi.org/10.1016/j.rse.2016.02.054

Goenka, R., Thakur, J., Taori, A., Bothale, R. V., & Chauhan, P. (2024). The prevailing smog conditions over the Delhi-NCR during the 2022 post monsoon. *Advances in Space Research*, *73*(5), 2609–2617. https://doi.org/10.1016/j.asr.2023.12.018

Han, Y., Revercomb, H., Cromp, M., Gu, D., Johnson, D., Mooney, D., et al. (2013). Suomi NPP CrIS measurements, sensor data record algorithm, calibration and validation activities, and record data quality. *Journal of Geophysical Research: Atmospheres*, *118*(22), 12734–12748. https://doi.org/10.1002/2013JD020344

Hersbach, H., Bell, B., Berrisford, P., Biavati, G., Horányi, A., Muñoz Sabater, J., et al. (2023). ERA5 hourly data on pressure levels from 1940 to present. *Copernicus Climate Change Service (C3S) Climate Data Store (CDS)*. https://doi.org/10.24381/cds.bd0915c6

Hersbach, H., Bell, B., Berrisford, P., Hirahara, S., Horányi, A., Muñoz-Sabater, J., et al. (2020). The ERA5 global reanalysis. *Quarterly Journal of the Royal Meteorological Society*, *146*(730), 1999–2049. https://doi.org/10.1002/qj.3803

Holloway, T., Levy II, H., & Kasibhatla, P. (2000). Global distribution of carbon monoxide. *Journal of Geophysical Research*, *105*(D10), 12123–12147. https://doi.org/10.1029/1999JD901173

Hurtmans, D., Coheur, P.-F., Wespes, C., Clarisse, L., Scharf, O., Clerbaux, C., et al. (2012). FORLI radiative transfer and retrieval code for IASI. *Journal of Quantitative Spectroscopy and Radiative Transfer*, *113*(11), 1391–1408. https://doi.org/10.1016/j.jqsrt.2012.02.036

Indian National Commission on Population. (2020). *Population projections for India and States 2011–2036*. [Tech. Rep.]. Indian Ministry of Health and Family and welfare.

Jethva, H., Torres, O., Field, R. D., Lyapustin, A., Gautam, R., & Kayetha, V. (2019). Connecting crop productivity, residue fires, and air quality over Northern India. *Scientific Reports*, *9*(1), 1. https://doi.org/10.1038/s41598-019-52799-x

Kanawade, V. P., Srivastava, A. K., Ram, K., Asmi, E., Vakkari, V., Soni, V. K., et al. (2020). What caused severe air pollution episode of November 2016 in New Delhi? *Atmospheric Environment*, *222*, 117125. https://doi.org/10.1016/j.atmosenv.2019.117125

Kemanth, K., Singh, R., & Ignatious, S. M. (2024). *How can Punjab increase the adoption of crop residue management methods?* Council on Energy, Environment and Water. (CEEW).

Kerzenmacher, T., Dils, B., Kumps, N., Blumenstock, T., Clerbaux, C., Coheur, P.-F., et al. (2012). Validation of IASI FORLI carbon monoxide retrievals using FTIR data from NDACC. *Atmospheric Measurement Techniques*, *5*(11), 2751–2761. https://doi.org/10.5194/amt-5-2751-2012

Kumari, S., Lakhani, A., & Kumari, K. M. (2021). Variation of carbon monoxide at a suburban site in the Indo-Gangetic Plain: Influence of long-range transport from crop residue burning region. *Atmospheric Pollution Research*, *12*(9), 101166. https://doi.org/10.1016/j.apr.2021.101166

Kumari, S., Verma, N., Lakhani, A., & Kumari, K. M. (2021b). Severe haze events in the Indo-Gangetic Plain during post-monsoon: Synergetic effect of synoptic meteorology and crop residue burning emission. *Science of The Total Environment*, *768*, 145479. https://doi.org/10.1016/j.scitotenv.2021.145479

Lan, R., Eastham, S. D., Liu, T., Norford, L. K., & Barrett, S. R. H. (2022). Air quality impacts of crop residue burning in India and mitigation alternatives. *Nature Communications*, *13*(1), 6537. https://doi.org/10.1038/s41467-022-34093-z

Landgraf, J., aan de Brugh, J., Scheepmaker, R., Borsdorff, T., Hu, H., Houweling, S., et al. (2016). Carbon monoxide total column retrievals from TROPOMI shortwave infrared measurements. *Atmospheric Measurement Techniques*, *9*(10), 4955–4975. https://doi.org/10.5194/amt-9-4955-2016

Langerock, B. (2023). *Validation report of reprocessed IASI L2 CO CDR for Metop-A and B*. [Tech. Rep.]. *EUMETSAT, AC SAF*. https://acsaf.org/docs/vr/Validation_Report_IASI_CO_CDR_Nov_2023.pdf

Lelieveld, J., Gromov, S., Pozzer, A., & Taraborrelli, D. (2016). Global tropospheric hydroxyl distribution, budget and reactivity. *Atmospheric Chemistry and Physics*, *16*(19), 12477–12493. https://doi.org/10.5194/acp-16-12477-2016

Li, F., Zhang, X., & Kondragunta, S. (2020). Biomass burning in Africa: An investigation of fire radiative power missed by MODIS using the 375 m VIIRS active fire product. *Remote Sensing*, *12*(10), 1561. Article 10. https://doi.org/10.3390/rs12101561

Liu, T., Mickley, L., Gautam, R., Singh, M., DeFries, R., & Marlier, M. (2019). Detection of delay in post-monsoon agricultural burning across Punjab, India: Potential drivers and consequences for air quality. https://eartharxiv.org/repository/view/1054/

Lopes, A. A., Tasneem, D., & Viriyavipart, A. (2023). Determinants of wheat residue burning: Evidence from India. *PLoS One*, *18*(12), e0296059. https://doi.org/10.1371/journal.pone.0296059

Ministry of Agriculture and Farmers Welfare, Government of India. (2023). *Agricultural statistics at a glance*. Department of Agriculture and Farmers Welfare, Government of India.

Majeed, R., Anjum, M. S., Imad-ud-din, M., Malik, S., Anwar, M. N., Anwar, B., & Khokhar, M. F. (2024). Solving the mysteries of Lahore smog: The fifth season in the country. *Frontiers in Sustainable Cities*, *5*, 1314426. https://doi.org/10.3389/frsc.2023.1314426

Mehta, C. R., & Badegaonkar, U. R. (2023). *Sustainable management of crop residues in Bangladesh, India, Nepal and Pakistan: Challenges and solutions* (South and South-West Asia development papers 23-01). *Centre for Sustainable Agricultural Mechanization (CSAM),Economic and Social Commission for Asia and Pacific (ESCAD), United Nations South and South-West Asia Office*.

Mushtaq, F., Farooq, M., Lala, M. G. N., Banerjee, S., Tirkey, A. S., Shaheen, F., & Meraj, G. (2024). Analysis of spatial variability of smog episodes over National Capital Delhi during (2013–2017). *Discover Applied Sciences*, *6*(8), 413. https://doi.org/10.1007/s42452-024-06109-4

Nandi, I., Srivastava, S., Yarragunta, Y., Kumar, R., & Mitra, D. (2020). Distribution of surface carbon monoxide over the Indian subcontinent: Investigation of source contributions using WRF-Chem. *Atmospheric Environment*, *243*, 117838. https://doi.org/10.1016/j.atmosenv.2020.117838

NASA MODIS Science Data Support Team. (2021). MODIS/Aqua+Terra Thermal Anomalies/Fire locations 1km FIRMS V0061 NRT (Vector data) [Dataset]. *NASA LANCE MODIS at the MODAPS*. https://doi.org/10.5067/FIRMS/MODIS/MCD14DL.NRT.0061

Nirmalkar, J., & Deb, M. K. (2016). Impact of intense field burning episode on aerosol mass loading and its possible health implications in rural area of eastern central India. *Air Quality, Atmosphere and Health*, *9*(3), 241–249. https://doi.org/10.1007/s11869-015-0330-y

Pakistan Bureau of Statistics. (2023). *Annoucement of results of 7th population and housing census*. [Tech. Rep.]. Government of Pakistan.

Pal, L., Ojha, C. S. P., & Dimri, A. P. (2021). Characterizing rainfall occurrence in India: Natural variability and recent trends. *Journal of Hydrology*, *603*, 126979. https://doi.org/10.1016/j.jhydrol.2021.126979

Pandey, A. K., Mishra, A. K., Kumar, R., Berwal, S., Devadas, R., Huete, A., & Kumar, K. (2017). CO variability and its association with household cooking fuels consumption over the Indo-Gangetic plains. *Environmental Pollution*, *222*, 83–93. https://doi.org/10.1016/j.envpol.2016.12.080

21698996, 2026, 4, Downloaded from https://agupubs.onlinelibrary.wiley.com/doi/10.1029/2025JD044219 by Bibliothèque de Sorbonne Université, Wiley Online Library on [19/02/2026]. See the Terms and Conditions (https://onlinelibrary.wiley.com/terms-and-conditions) on Wiley Online Library for rules of use; OA articles are governed by the applicable Creative Commons License

Parihar, D. S., Narang, M. K., Dogra, B., Prakash, A., & Mahadik, A. (2023). Rice residue burning in Northern India: An assessment of environmental concerns and potential solutions – A review. *Environmental Research Communications*, *5*(6), 062001. https://doi.org/10.1088/2515-7620/acb6d4

Pati, I. (2024). *Farm fires down since '20, but NCR's air not cleared as much*. The Times of India. Retrieved from https://timesofindia.indiatimes.com/city/gurgaon/stubble-burning-decreases-in-punjab-and-haryana-yet-delhi-ncr-air-quality-remains-poor/articleshow/115392746.cms

Potdar, S. S., Siingh, D., & Singh, R. P. (2024). Long-term study of spatial and temporal variations in biomass burning over the Indian region using MODIS products. *Journal of Earth System Science*, *133*(3), 129. https://doi.org/10.1007/s12040-024-02351-x

Ravindra, K., Singh, T., & Mor, S. (2022). COVID-19 pandemic and sudden rise in crop residue burning in India: Issues and prospects for sustainable crop residue management. *Environmental Science and Pollution Research*, *29*(2), 3155–3161. https://doi.org/10.1007/s11356-021-17550-y

Reddy, C. S., Unnikrishnan, A., Bird, N. G., Faseela, V. S., Asra, M., Manikandan, T. M., & Rao, P. V. N. (2020). Characterizing Vegetation Fire dynamics in Myanmar and South Asian countries. *Journal of the Indian Society of Remote Sensing*, *48*(12), 1829–1843. https://doi.org/10.1007/s12524-020-01205-5

Research Institute for Humanity and Nature (RIHN). (2025). Aakash Project: Towards mitigating particulate air pollution for improved public health along with sustainable agriculture in Northwest India. Retrieved from https://aakash-rihn.org/en/final-report/

Roy, C., Ayantika, D. C., Girach, I., & Chakrabarty, C. (2022). Intense biomass burning over Northern India and its impact on air quality, chemistry and climate. In P. Saxena, A. Shukla, & A. K. Gupta (Eds.), *Extremes in atmospheric processes and phenomenon: Assessment, impacts and mitigation* (pp. 169–204). Springer Nature. https://doi.org/10.1007/978-981-16-7727-4_8

Sahu, S. K., Mangaraj, P., Beig, G., Samal, A., Chinmay, P., Dash, S., & Tyagi, B. (2021). Quantifying the high resolution seasonal emission of air pollutants from crop residue burning in India. *Environmental Pollution*, *286*, 117165. https://doi.org/10.1016/j.envpol.2021.117165

Sawlani, R., Agnihotri, R., Sharma, C., Patra, P. K., Dimri, A. P., Ram, K., & Verma, R. L. (2019). The severe Delhi SMOG of 2016: A case of delayed crop residue burning, coincident firecracker emissions, and atypical meteorology. *Atmospheric Pollution Research*, *10*(3), 868–879. https://doi.org/10.1016/j.apr.2018.12.015

Sembhi, H., Wooster, M., Zhang, T., Sharma, S., Singh, N., Agarwal, S., et al. (2020). Post-monsoon air quality degradation across Northern India: Assessing the impact of policy-related shifts in timing and amount of crop residue burnt. *Environmental Research Letters*, *15*(10), 104067. https://doi.org/10.1088/1748-9326/aba714

Sharma, A., Srivastava, S., Kumar, R., & Mitra, D. (2024). Source attribution of carbon monoxide over Northern India during crop residue burning period over Punjab. *Environmental Pollution*, *359*, 124707. https://doi.org/10.1016/j.envpol.2024.124707

Sharma, D., & Mauzerall, D. (2022). Analysis of Air Pollution Data in India between 2015 and 2019. *Aerosol and Air Quality Research*, *22*(2), 210204. https://doi.org/10.4209/aaqr.210204

Singh, N., Agarwal, S., Sharma, S., Chatani, S., & Ramanathan, V. (2021). Air pollution over India: Causal factors for the high pollution with implications for mitigation. *ACS Earth and Space Chemistry*, *5*(12), 3297–3312. https://doi.org/10.1021/acsearthspacechem.1c00170

Singh, R., Sharma, C., & Agrawal, M. (2017). Emission inventory of trace gases from road transport in India. *Transportation Research Part D: Transport and Environment*, *52*, 64–72. https://doi.org/10.1016/j.trd.2017.02.011

Singh, Y., & Sidhu, H. S. (2014). Management of cereal crop residues for sustainable rice-wheat production System in the indo-gangetic plains of India. *Proceedings of the Indian National Science Academy*, *80*(1), 95. https://doi.org/10.16943/ptinsa/2014/v80i1/55089

Stein, A. F., Draxler, R. R., Rolph, G. D., Stunder, B. J. B., Cohen, M. D., & Ngan, F. (2015). NOAA's HYSPLIT atmospheric transport and dispersion modeling System. *Bulletin of the American Meteorological Society*, *96*(12), 2059–2077. https://doi.org/10.1175/BAMS-D-14-00110.1

Turquety, S., Hurtmans, D., Hadji-Lazaro, J., Coheur, P.-F., Clerbaux, C., Josset, D., & Tsamalis, C. (2009). Tracking the emission and transport of pollution from wildfires using the IASI CO retrievals: Analysis of the summer 2007 Greek fires. *Atmospheric Chemistry and Physics*, *9*(14), 4897–4913. https://doi.org/10.5194/acp-9-4897-2009

Vadrevu, K., & Lasko, K. (2018). Intercomparison of MODIS AQUA and VIIRS I-Band fires and emissions in an agricultural Landscape—Implications for air pollution research. *Remote Sensing*, *10*(7), 978. Article 7. https://doi.org/10.3390/rs10070978

Vadrevu, K. P., Giglio, L., & Justice, C. (2013). Satellite based analysis of fire–carbon monoxide relationships from forest and agricultural residue burning (2003–2011). *Atmospheric Environment*, *64*, 179–191. https://doi.org/10.1016/j.atmosenv.2012.09.055

Vadrevu, K. P., Lasko, K., Giglio, L., Schroeder, W., Biswas, S., & Justice, C. (2019). Trends in vegetation fires in South and Southeast Asian countries. *Scientific Reports*, *9*(1), 7422. https://doi.org/10.1038/s41598-019-43940-x

Veefkind, J. P., Aben, I., McMullan, K., Förster, H., de Vries, J., Otter, G., et al. (2012). TROPOMI on the ESA Sentinel-5 precursor: A GMES mission for global observations of the atmospheric composition for climate, air quality and ozone layer applications. *Remote Sensing of Environment*, *120*, 70–83. https://doi.org/10.1016/j.rse.2011.09.027

Wang, X., Folberth, C., Skalsky, R., Wang, S., Chen, B., Liu, Y., et al. (2022). Crop calendar optimization for climate change adaptation in rice-based multiple cropping systems of India and Bangladesh. *Agricultural and Forest Meteorology*, *315*, 108830. https://doi.org/10.1016/j.agrformet.2022.108830

21698996, 2026, 4, Downloaded from https://agupubs.onlinelibrary.wiley.com/doi/10.1029/2025JD044219 by Bibliothèque de Sorbonne Université, Wiley Online Library on [19/02/2026]. See the Terms and Conditions (https://onlinelibrary.wiley.com/terms-and-conditions) on Wiley Online Library for rules of use; OA articles are governed by the applicable Creative Commons License